

## ORIGINAL ARTICLE

# Nothing to lose? Neural correlates of decision, anticipation, and feedback in the balloon analog risk task

Stephanie N. L. Schmidt  | Sarah Sehrig | Alexander Wolber | Brigitte Rockstroh | Daniela Mier 

Department of Psychology, University of Konstanz, Konstanz, Germany

## Correspondence

Stephanie N. L. Schmidt, Department of Psychology, University of Konstanz, Universitaetsstrasse 10, Box 905, 78457 Konstanz, Germany.

Email: [stephanie.3.schmidt@uni-konstanz.de](mailto:stephanie.3.schmidt@uni-konstanz.de)

## Funding information

Deutsche Forschungsgemeinschaft, Grant/Award Number: GZ: MI 1975/7-1

## Abstract

Understanding the subprocesses of risky decision making is a prerequisite for understanding (dys-)functional decisions. For the present fMRI study, we designed a novel variant of the balloon-analog-risk task (BART) that measures three phases: decision making, reward anticipation, and feedback processing. Twenty-nine healthy young adults completed the BART. We analyzed neural activity and functional connectivity. Parametric modulation allowed assessing changes in brain functioning depending on the riskiness of the decision. Our results confirm involvement of nucleus accumbens, insula, anterior cingulate cortex, and dorso-lateral prefrontal cortex in all subprocesses of risky decision-making. In addition, subprocesses were differentiated by the strength of activation in these regions, as well as by changes in activity and nucleus accumbens-connectivity by the riskiness of the decision. The presented fMRI-BART variant allows distinguishing activity and connectivity during the subprocesses of risky decision making and shows how activation and connectivity patterns relate to the riskiness of the decision. Hence, it is a useful tool for unraveling impairments in subprocesses of risky decision making in people with high risk behavior.

## KEYWORDS

BART, fMRI, probabilistic, risky decision making, ventral striatum

## 1 | INTRODUCTION

At the core of human behavior lies our remarkable ability to make choices, even when we are uncertain about the outcomes. To truly grasp how people take risks, both in healthy and problematic ways, it is crucial to uncover the neural mechanisms that guide these decisions. Over the last decades, the balloon analog risk task (BART) has served as a cornerstone in exploring the interplay between

behavior and neural processes of risky decision making. However, the traditional BART design does not allow distinguishing between decision and outcome anticipation. Understanding the intricate interplay of behavioral and neural factors in risky decision making depends on our ability to precisely dissect these subprocesses. Here, we present a novel variant of the BART that allows distinguishing decision, anticipation, and feedback phase by *their neural activity and connectivity*.

This is an open access article under the terms of the [Creative Commons Attribution-NonCommercial-NoDerivs](https://creativecommons.org/licenses/by-nc-nd/4.0/) License, which permits use and distribution in any medium, provided the original work is properly cited, the use is non-commercial and no modifications or adaptations are made.

© 2024 The Author(s). *Psychophysiology* published by Wiley Periodicals LLC on behalf of Society for Psychophysiological Research.

The BART has been proposed as a measure of real-world risk taking behavior (Helfinstein et al., 2014; Schonberg et al., 2012). Virtual balloons are pumped up via button presses, with monetary gain rewarding every successful pump. Gain is secure in the “cash out” option, while accidental balloon popping leads to the loss of the accumulated gain in the respective trial. Thus, each inflation is a risky decision, and with each pump the risk of explosion and the uncertainty of a gain increases. The BART design takes into account the sequential process of decision making: The outcome of previous inflations; i.e., feedback, the decision to further inflate the balloon or to cash out, and the anticipation of reward feedback. The feedback can either be an expected reward in cash-out trials, an uncertain reward in consequence of successful inflation, or an unexpected loss in consequence of unsuccessful inflation. This combination of perceiving the growing balloon size as rewarding on the one hand, and at the same time realizing the increasing probability of loss on the other hand, leads to increasing emotional tension during anticipation of the feedback. This relates choice behavior in the BART to naturalistic risk behaviors like alcohol consumption, smoking, stealing, and drug use (Bornovalova et al., 2005; Lejuez, Aklin, Jones, et al., 2003; Lejuez, Aklin, Zvolensky, & Pedulla, 2003; Lejuez et al., 2002), as well as to sensation seeking and impulsivity (Lauriola et al., 2013). With decisions to inflate or cash out, anticipation of a reward, and processing of the feedback, three major functionally and temporally related components emerge as integral parts of decision making, which may be modulated by the decision risk—and which should, as we hypothesize, become manifest in distinct activity and connectivity patterns. The present BART-variant was designed to substantiate this hypothesis.

Several cortical and subcortical structures have been identified as involved in (risky) decision making. The mesocorticolimbic system (Rausch et al., 2014, 2015; Schmidt et al., 2019) with its dopaminergic ascending projections constitutes the central part of the reward system and is essential for behavioral motivation and goal-directed behavior (Koob, 1996; Salamone & Correa, 2012). Moreover, frontal and prefrontal structures have been associated with the cognitive-emotional aspects of decision making and reward processing, in particular the anterior cingulate cortex (ACC), ventromedial (vmPFC), dorsolateral prefrontal cortex (DLPFC), and insula (Dolcos et al., 2011; Naqvi et al., 2006).

The ventral striatum as core of the mesocorticolimbic system, including the nucleus accumbens (Nacc), is considered central to the processing of stimulus salience (Schmidt et al., 2019; Zink et al., 2004), reward-prediction, and reward-guided behavior (Burton et al., 2015, 2018; Malvaez & Wassum, 2018). Higher striatal activity was

linked to riskier rather than less risky decisions in the BART (Claus & Hutchison, 2012; Wang et al., 2022). Further, the ventral striatum has been reported to be active in the BART during reward feedback processing (Schonberg et al., 2012). In addition, increased striatal activity was observed during loss feedback compared to (rewarding) cash-out feedback and might reflect prediction error and stimulus salience during unexpected loss (Rao et al., 2008). However, a worse than expected outcome, i.e., negative prediction error, should lead to reduced dopamine signaling, whereas better than expected outcome, i.e., positive prediction error, should lead to increased dopamine signaling (Schultz, 2016). Thus, results about striatal activity upon loss feedback remain inconclusive. Moreover, potentially distinct roles of the Nacc in reward anticipation and decision making in the BART remain unclear. Consequently, to date it has not been experimentally shown, whether Nacc-activation during the decision for or against an inflation of the balloon reflects the decision itself or the anticipation of a reward.

Nacc maintains functional connections to the DLPFC (Becker et al., 2017; Kohno et al., 2014) which is considered relevant for maintaining and manipulating cognitive representations, planning future actions (Manes et al., 2002; Miller & Cohen, 2001), and cognitive control by suppressing risky responses (Fecteau et al., 2007; Telzer et al., 2013). Decision making during riskier trials in the BART is linked to augmented DLPFC activity (Rao et al., 2008; Schonberg et al., 2012), possibly because decision evaluation requires more control. Further, individuals, who made riskier decisions in the BART, had less DLPFC activity and reduced coupling between DLPFC and subcortical affective regions like insula and striatum, which was discussed as a sign of cortical–subcortical imbalance (Telzer et al., 2013). Accordingly, enhanced DLPFC activation by transcranial direct current stimulation prompted reduced risk taking in the BART (Fecteau et al., 2007).

Conclusions about the role of (vm)PFC and the orbitofrontal cortex (OFC) in decision making have also been drawn from dysfunctional decision making in individuals with alcohol use disorders and subjects with vmPFC damage (Bechara et al., 2001; Fellows & Farah, 2007). In simple decision making tasks, the lateral part of the prefrontal cortex has been linked to (risky) decision making and the processing of loss feedback, while medial and orbitofrontal parts were mainly active during the processing of reward feedback and reward anticipation (Kahnt et al., 2010; Knutson, Fong, et al., 2001; Ströhle et al., 2008). Uncertain gain in the BART was associated with increased mPFC activity, which was further modulated by riskiness; i.e., probability of explosion (Bogg et al., 2012). Moreover, vmPFC activity was also reported during risky decision making in

the BART (Bogg et al., 2012; Fukunaga et al., 2012). It has been concluded that in particular when reward feedback becomes less predictable, mPFC activity reflects salience (Euston et al., 2012), reward seeking (Bogg et al., 2012), and cognitive control, as well as estimation of error likelihood of decisions (Alexander & Brown, 2010).

Regarding limbic brain regions, the contribution of the ACC to risky decision making is related to its role in reinforcement learning, when actual and expected decision and behavioral feedback is compared and error likelihood of decisions and behavior is updated (Holroyd & Coles, 2002). Through its connection with lateral prefrontal areas, the ACC is associated with cognitive control to avoid risks (Brown & Braver, 2007). Indeed, lower ACC activity during risky decisions in the BART was found to correlate with harmful drinking which might reflect reduced ability to anticipate negative outcome of risky behavior (Claus & Hutchison, 2012). Insula activity is commonly associated with the processing of negative or aversive emotions (Steward et al., 2016), but was also present during risky decisions in the BART (Burnette et al., 2021; Korucuoglu et al., 2020), and as the ACC, insula activity has been associated with risk and loss aversion (Markett et al., 2016). Consequently, insula activity was reported following losses compared to cash-out feedback (Rao et al., 2008). Finally, riskier decisions after loss compared to cash-out feedback were associated with increased amygdala and hippocampus modulation (Kohn et al., 2015). Importantly, to our knowledge, augmented ACC and insula activity during the anticipation of reward feedback in decision making tasks has not been reported, which supports our hypothesis that activity patterns distinguish the components of (risky) decision making.

Taken together, Nacc activity characterizes reward anticipation and (risky) decision making (Burton et al., 2018; Claus & Hutchison, 2012; Walter, 2003), but is not consistently reported following feedback in the BART. OFC and mPFC-activity seem to vary with reward anticipation and reward feedback processing, while lateral PFC activity has been reported for (risky) decisions and the processing of loss feedback and ACC and insula for loss feedback and risk aversion.

Thus, despite the substantial evidence of close interaction of the mentioned cortical and subcortical structures in the complex, sequential process of decision making, apparently individual activity patterns seem to indicate distinct functional significance of specific structures for the subprocesses of decision making. In order to substantiate this assumption, the BART-variant was modified to allow the measurement of brain activity and connectivity patterns during decisions, anticipation, and feedback processing. Notwithstanding that these subprocesses of decision making are temporally and functionally related, this was

achieved by a multipart trial that in addition to previous versions of the BART has not only subphases for decision making and for the feedback but also an additional sub-phase for anticipation.

We assume to find activation in Nacc during decision making. In addition, with increasing risk of the decision, we expect decreased connectivity between Nacc and prefrontal regions, as well as increased amygdala and insula activation. For anticipation and for reward feedback, we also assume activation in Nacc. For loss feedback insula and amygdala activity are expected and a decrease in Nacc activation.

These hypotheses are part of our pre-registration on open science framework (<http://osf.io/b6uf5>). All further reported activity and connectivity analyses within and between the subprocesses of risky decision making are exploratory because the current state of literature does not allow firm conclusions.

## 2 | METHOD

### 2.1 | Participants

Thirty-six volunteers were recruited via an online platform of the University of Konstanz (Sona) or personal contacts of the study team. Inclusion criteria were right-handedness (according to the participants answers to a one-item question on handedness), MRI compatibility, and mental health. Mental health was verified by the telephone version of the Structured Clinical Interview for DSM-5 Disorders–Clinician Version (SCID-5-CV) interview (Beesdo-Baum et al., 2019). The SCID-5-CV screens for present and past psychopathology according to DSM 5 standards. Specifically, it assesses alcohol and substance use disorder, depressive disorder, bipolar disorder, psychotic/schizophrenic disorder, eating disorders, anxiety disorders, obsessive–compulsive disorders and also includes questions addressing the presence of additional mental health concerns and allowing for open-ended responses. Individuals for whom mental health according to the SCID-5-CV could not be verified were not included in this study.

All participants had higher education entrance certification (at least 12 years of school education), sufficient command of the German language, and normal or corrected-to-normal vision (participants with myopia or hyperopia received MRI-compatible glasses for the tasks).  $N = 7$  participants did not accomplish the entire measurements that consisted of 2 fMRI appointments (reasons for drop-out were: not finding time for the second appointment of the study ( $n = 4$ ), invariable, stereotypic choice behavior in the BART, i.e., cashing out too soon, leading to no

or at most one burst balloon, which does not allow calculation of the according fMRI contrasts ( $n=2$ ), withdrawal from the entire study due to dissatisfaction with the tasks ( $n=1$ ), so that datasets of  $n=29$  participants (18 women, 11 men, mean age:  $23.14 \pm 2.94$  years, range 18–28 years) were available for analyses.

## 2.2 | Procedure

Interested volunteers participated in a 30-min telephone interview in which they were screened for MRI compatibility and mental health and were informed about study procedures and aims; i.e., investigating how risk is perceived and how one reacts to perceived risk. As the study took place during the COVID-19 pandemic, infection risk and status were also inquired. Volunteers meeting the eligibility criteria were invited to two appointments 3–5 weeks apart. The mean number of days between the appointments was 29.3 days (standard deviation 3.6; range 21–37). As the data were collected during the COVID-19 pandemic (August–December 2020), participants had to follow the local regulations, including wearing a face mask and getting their body temperature measured when entering the MRI facility (Neurological Rehabilitation Center Schmieder Clinic, Allensbach, Germany). The study has been approved by the ethics board of the University of Konstanz.

The first appointment started with further information about the tasks and measurements. Participants completed the MRI safety checklist, signed written informed consent, and practiced the tasks on a laptop using a response pad similar to the one during the MRI-measurement.

Both appointments were identical with respect to the 45–50 min MRI session with the BART and a trustworthiness evaluation task that is reported elsewhere and a post-experimental rating. The first appointment also had a questionnaire set on personality traits and emotion processing. Participants received a compensation of 20 € per session in addition to the monetary gain of each BART (see details below).

## 2.3 | Experimental task: Balloon analog risk task (BART) variant

In the novel BART variant, participants see a small balloon on the monitor and decide to pump it up or to cash out. Decision making considers the sequential processes of previous inflations, including (1) the decision to further inflate the balloon or to cash out, (2) the subsequent anticipation of a gain, and (3) feedback processing. Feedback varies between (a) expected reward feedback (cash out),

(b) uncertain reward feedback upon pump decision, and (c) unexpected loss feedback (balloon popping following the decision to further inflate the balloon). While the risk of explosion increases with each inflation, reward also increases with each successful inflation. Reward feedback within a trial is signaled by adding 0.25 € gain to the total monetary gain balance and the next size balloon on the monitor. If a balloon explodes before choosing to cash out, the accumulated money of the trial is lost. The present BART, in comparison to previous versions, has a separate anticipation phase between the decision and the feedback.

Within a series of 12 trials, each trial starts with a 3-s decision phase, in which a small green balloon is presented in the middle of the screen with the two decision options “inflate” (German: “aufpumpen”) and “cash out” (German: “auszahlen”) displayed beneath it (Figure 1). Participants are instructed that they should decide for each balloon whether they want to pump up or cash out. They are also instructed that each successful pump (no popping) is rewarded by 25 Cents, but that the accumulated gain of the trial is lost in case of explosion, and that the risk of balloon popping increases with size thus, with each pump. Participants are told to indicate their decision choice by pressing the left or right button on the keypad with the thumb of their right hand, and if they do not respond within the 3-s period, the option “inflate” is selected automatically. The decision phase is followed by a jittered inter-stimulus-interval (ISI) of 1–5 s, in which the fixation cross appears in the middle of the screen. Then, without response options, the same size balloon as in the decision phase is presented for 2 s in the anticipation phase, again followed by a jittered 1–5 s ISI. The final 2-s feedback phase is either an expected reward feedback (cash out option) that is illustrated by a golden colored balloon in the middle of the screen together with the word “reward” (German: “Gewinn!”) underneath, an uncertain reward (upon pump decision), illustrated by the next-sized green balloon together with the word “reward” beneath (German “Gewinn!”), or unexpected loss feedback with a red burst balloon with “loss” written beneath (German: “Verlust!”). At the end of a trial, the total gain within the trial and the total balance accumulated over all trials are presented for 2 s. In addition to these experimental trials, there are control trials with null events. Specifically, alternating with the experimental trials, there are fixation crosses lasting for approximately 30 s, which include ITIs, ISIs, and one null event per condition.

Each trial comprises 9 balloons: the first presentation and up to 8 inflations by the participant. The probability of explosion linearly increases with each trial from zero to 8/9. The randomization for the explosion was implemented as follows: For each trial, there was a logical vector of length 9. For the first trial, the vector contained eight

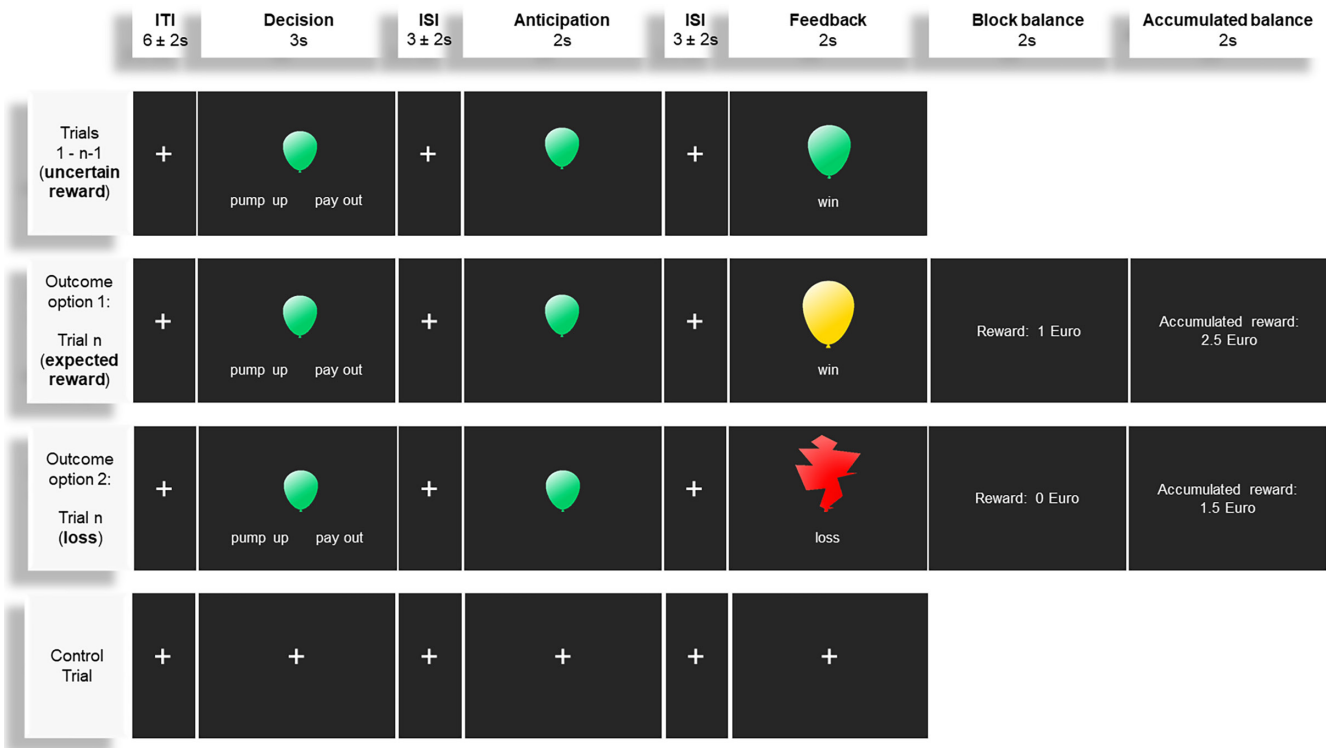


**FIGURE 1** BART paradigm flow, first three lines are possible steps of each experimental trial, fourth line is the control trial comprising null events in form of fixation crosses for each condition. The reward of 1€ indicates cashing out after the 4th balloon with each giving 25 Cent.

times false and once true, i.e., 1/9 probability of bursting. The ratio of false and true increased with each trial. Then, for each trial, the vector was randomly shuffled, and the value at the first position was considered. If it was true, the balloon would burst in the current round, if it was false, another inflation was possible.

Based on a simulation with a custom-made MATLAB script and using 100,000 balloons, our randomization algorithm leads to an explosion after an average of 3.4 inflations.

## 2.4 | Data acquisition

fMRI measurements took place at the Neurological Rehabilitation Center Schmieder Clinic, Allensbach, with a 3T Siemens Skyra MRI and Syngo MR D13 software, using a 32-channel coil. First, anatomical images were acquired using an MPRage protocol with a slice thickness of 1 mm, repetition time 2.5 s, echo time 4.06 ms, field of view 256 mm, flip angle 7°, and 192 slices. Participants watched a nature movie during all measurements preceding the first task. During the tasks, blood-oxygen level-dependent brain signals were measured using echo-planar imaging with 38 interleaved slices, with a slice thickness of 3.4 mm and no gap. Repetition time was 2.5 s, echo time 30 ms, flip angle 80°, matrix 64 × 64, and field of view 218 mm. A

maximum of 800 volumes could be measured, but since experiment time was dependent on individual response behavior, the sequence was manually stopped at the end of the experiment. Regions of interest were the left and right anterior cingulate cortex (left: 400 voxels; right: 362 voxels, taken from the Neuromorphometrics, Inc. Atlas (Bakker et al., 2015)); left and right insula (left: 592 voxels; right 492 voxels, taken from MARINA (Walter, 2003)); left and right nucleus accumbens (left: 51 voxels; right: 44 voxels, taken from AAL3 (Rolls et al., 2020)); medial prefrontal cortex (1431 voxels, union of medial superior frontal and orbital superior frontal regions in MARINA), dorsolateral prefrontal cortex (left: 228 voxels, right: 373 voxels, union of BA9 and BA46 from WFU Pickatlas TD (Maldjian et al., 2003, 2004), with the medial parts removed), and amygdala (left: 84 voxels, right: 91 voxels, taken from Neuromorphometrics, Inc. Atlas (Bakker et al., 2015)).

Experimental paradigms were programmed and presented using presentation (Version 21.1 Build 09.05.19, Neurobehavioral Systems, Inc., [www.neurobs.com](http://www.neurobs.com)). Participants gave their responses on a diamond-shaped 4-button Lumina response pad LS-DIAM (Cedrus Design, [www.cedrus.com](http://www.cedrus.com)). The masks, as well as the BART presentation file and analysis scripts are available on <https://osf.io/pkbt6/>. In addition, we make the fMRI data (raw,

converted nifti-files of the EPIs) available upon request to researchers signing a data protection statement.

## 2.5 | Data analysis

Behavioral data were analyzed using custom scripts in MATLAB 2020b (version 9.9.0 (R2020b). Natick, Massachusetts: The MathWorks Inc.) and R (R Foundation for Statistical Computing, Vienna, Austria. <https://www.R-project.org>).

The average number of pumps of balloons that did not explode (“adjusted number of pumps”) was analyzed as a correlate of risky decision making (Lejuez, Aklin, Zvolensky, & Pedulla, 2003; Lejuez et al., 2002). fMRI data analysis was also performed using MATLAB 2020b (version 9.9.0 (R2020b). Natick, Massachusetts: The MathWorks Inc.) and with the Statistical Parametric Mapping 12 toolbox (SPM12, <https://www.fil.ion.ucl.ac.uk/spm/software/spm12/>).

Preprocessing included slice time correction to the middle slice, realignment to the mean image and unwarping, normalization with resampling to  $3 \times 3 \times 3$  mm voxel size, and smoothing with a 9 mm Gaussian kernel.

For the first-level models, an event-related design was chosen, and data were high-pass filtered at 512s. For standard activation analyses as preregistered on Open Science Framework (<https://osf.io/b6uf5>), a GLM with 8 regressors of interest was set-up: decision phase, the anticipation phase, the feedback phase (separated into expected reward feedback, unexpected loss feedback, and uncertain reward feedback), the null events, the accumulated winnings screen, and the participants' key presses. In addition, six movement parameters from the realignment procedure served as regressors of no interest. Duration of all events was set to 0s.

Based on these regressors, we set up the following contrasts: decision making > null, reward anticipation > null, uncertain reward feedback > null, expected reward feedback > null, unexpected loss feedback > null, rewards > null, expected reward feedback > unexpected loss feedback, decision making > reward anticipation, decision making > uncertain reward feedback, decision making > expected reward feedback, uncertain reward feedback > expected reward feedback, reward anticipation > expected reward feedback, reward anticipation > uncertain reward feedback, uncertain reward feedback > unexpected loss feedback.

In addition, creating of the parametric modulation parameters for each person at the first level was accomplished in 2 steps. First, each balloon presentation in each phase was numbered, starting with 1 for the lowest risk balloon in every trial, increasing by 1 for each subsequent

balloon within the trial. Second, the riskiness numbers were normalized to mean 1 for each subject in order to reduce correlations with the main regressor and to increase comparability of the parametric modulator over participants. For the results, we only consider the decision, anticipation, and uncertain rewards in trials for which the participants chose to pump up the balloon, because these conditions occur several times for each trial and have enough events for the parametric modulation (i.e., the final feedback screens are not analyzed with parametric modulation). Trials in which participants decided to cash out were omitted because they are followed by an expected reward and would therefore not represent the highest risk in a row.

To investigate brain-behavior relationships, we performed generalized psychophysiological interaction analyses (gPPI), which have been shown to have high sensitivity and specificity, also in tasks including more than 2 conditions (McLaren et al., 2012). The gPPI analyses are based on the first level models of regular activation analyses. Because we were interested in the connectivity changes depending on the riskiness of a trial, we based the gPPI analyses on the parametric modulation analyses. The durations were set to the response time during the decision events and to 2s (i.e., the duration of stimulus presentation) for the other conditions.

In the gPPI analysis, the eigenvariates of the seed regions were extracted at the default significance threshold of .5 to obtain a seed region time course from our ROIs. Deconvolution of the extracted neural signal leads to the estimated neural activity, which is then separately multiplied by the condition-specific regressors and finally convolved with the HRF.

gPPI analyses were performed on the decision, anticipation, and uncertain reward feedback events of the trials in which participants chose to inflate the balloon. Left and right Nacc were used as seed regions.

The second-level analyses were performed on the first-level contrasts using t-tests. Whole-brain activation data were considered at a significance threshold of  $p < .05$ , FWE-corrected, with a minimum cluster size  $k > 10$ . For parametric modulation, whole-brain activation, and gPPI results, we used  $p < .001$ , uncorrected,  $k > 10$ . All small-volume analyses were conducted at whole brain  $p < .05$ , with peak-level FWE-correction  $p < .05$ ,  $k > 10$ .

## 3 | RESULTS

### 3.1 | Decision behavior

Participants decided for balloon inflation on average 2.7 ( $\pm 0.6$ ) times per trial. Figure 2 displays the distribution of

the last inflation decisions for each trial and person, i.e., how often did a person inflate before cashing out or explosion. Considering only successful inflations that did not lead to an explosion of the balloon, the average adjusted number of pumps was 2.1 ( $\pm 0.7$ ). Of the 12 trials, the balloon exploded on average 4.5 ( $\pm 1.4$ ) times.

For inflation decisions leading to uncertain rewards, the average RT was 862 ms ( $\pm 227$  ms); for inflation decisions leading to unexpected losses, the average RT was 921 ms ( $\pm 410$  ms); and for expected reward decisions, the average RT was 717 ms ( $\pm 252$  ms). Paired-sample *t*-tests show significant differences between uncertain reward and expected reward decisions ( $p < .0001$ ) and between expected reward and unexpected loss decisions ( $p = .0011$ ), but not between uncertain reward with unexpected losses ( $p = .270$ ).

Due to the individual decision behavior, the average number of volumes collected during the MRI measurement was 428 ( $\pm 38$ ), resulting in an average experiment duration of approximately 18 min.

### 3.2 | fMRI activation patterns

Overall whole-brain results demonstrate strong effects of distinct activation patterns for the different decision processes: During decisions compared to null events, widespread increased activation includes insula, thalamus, and striatum.

Anticipation compared to null events increased activation mainly in insula, inferior prefrontal, and inferior

frontal gyrus. Feedback prompted another distinction of prominent activation patterns: For uncertain rewards compared to null events, stronger activation was measured in mPFC, insula, inferior parietal lobe, thalamus, striatum.

Expected rewards relative to null events were associated with increased activation in a large cluster spanning fusiform gyrus and visual association cortex, whereas unexpected losses are associated with stronger activation in inferior prefrontal gyrus reaching into insula and dorsal ACC. Activation is decreased during unexpected losses compared to the null events in pre-motor and primary motor areas.

For detailed results, please refer to [Table 1](#) for whole-brain and [Table 2](#) for small-volume corrected results, and for a visualization to [Figure 3](#).

In support of our hypotheses, small-volume correction confirmed increased activation in the bilateral Nacc for decision making, reward anticipation, and uncertain rewards relative to null events. In addition, conditions differ significantly in that decision making prompts the strongest bilateral Nacc activation, uncertain rewards medium Nacc activation, and reward anticipation the lowest Nacc activation compared to the other two phases. No significant Nacc activation is confirmed during expected reward feedback. The expectation of a negative association of unexpected loss feedback (relative to null events) with Nacc activation was not confirmed. In contrast, there was a positive association of unexpected loss feedback with Nacc activation (see [Figure 4](#) boxplots). In line with the

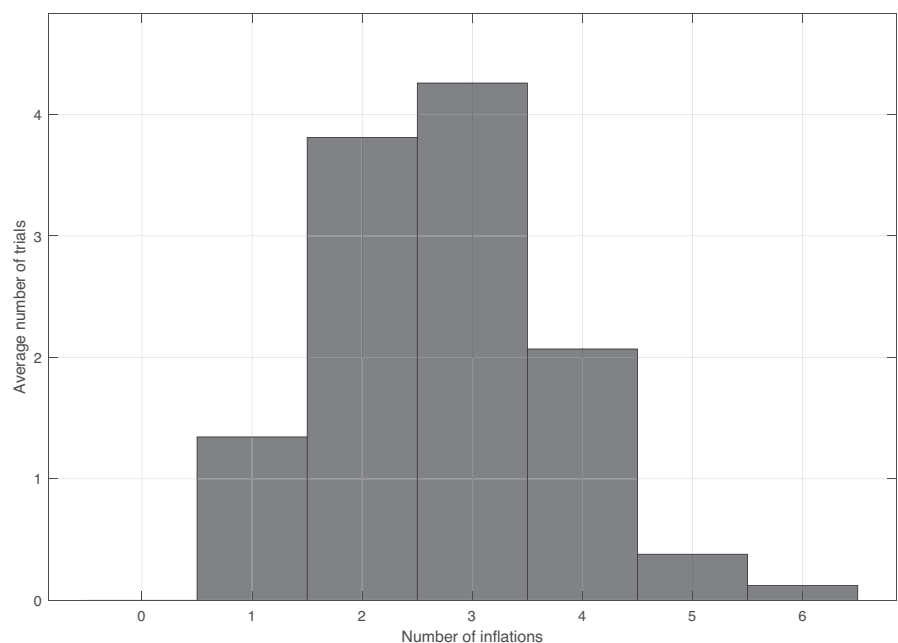


**FIGURE 2** Distribution of balloon inflation frequencies across participants.

TABLE 1 Activation: Whole brain.

Area	Hemisphere	BA	Cluster	MNI			t-value
				x	y	z	
Decision making >0							
Cerebellum	Right		15,263	27	-55	-19	17.28
Somatosensory Cortex	Left	3		-45	-19	56	16.66
Primary Motor Cortex	Left	4		-36	-31	65	16.11
Frontopolar area	Left	10	144	-30	41	23	9.01
Dorsolateral prefrontal cortex	Left	9		-33	38	35	6.97
Frontopolar area	Right	10	162	33	47	20	7.81
Dorsolateral prefrontal cortex	Right	9		30	35	32	6.84
Dorsolateral prefrontal cortex	Right	9		24	32	26	6.66
Cerebellum	Left		40	0	-25	-40	7.50
Reward anticipation >0							
Fusiform gyrus	Left	37	602	-39	-52	-16	12.38
Visual association cortex	Left	19		-39	-67	-10	11.46
Cerebellum	Left			-39	-43	-28	8.74
Inferior prefrontal gyrus	Right	47	587	33	26	-7	10.58
Dorsolateral prefrontal cortex	Right	9		39	11	29	10.34
Inferior frontal gyrus, pars opercularis	Right	45		33	26	5	9.43
Insula	Left	13	112	-33	23	8	10.29
Inferior prefrontal gyrus	Left	47		-30	23	-4	9.39
Fusiform gyrus	Right	37	799	45	-49	-10	10.18
Visual association cortex	Right	19		30	-88	8	9.94
Visual association cortex	Right	19		33	-76	-7	9.77
Somatosensory association cortex	Left	7	90	-24	-55	41	9.07
Pre-motor and supplementary motor cortex	Left	6	72	-39	2	47	8.69
Dorsolateral prefrontal cortex	Left	9		-39	5	29	6.50
Somatosensory association cortex	Right	7	120	24	-52	44	7.41
Cerebellum	Left		20	-15	-73	-37	7.21
Uncertain reward >0							
Cerebellum	Left		3957	-42	-49	-31	12.38
Fusiform gyrus	Left	37		-39	-64	-7	11.94
Visual association cortex	Right	18		18	-94	17	11.81
Inferior prefrontal gyrus	Right	47	3084	27	32	2	10.33
Inferior prefrontal gyrus	Right	47		33	23	-10	10.00
Inferior prefrontal gyrus	Right	47		27	26	-4	9.96
Somatosensory association cortex	Left	7	461	-21	-55	44	9.86
Supramarginal gyrus	Left	40		-36	-31	47	8.55
Somatosensory cortex	Left	1		-54	-19	53	6.01
Dorsal posterior cingular cortex	Right	31	692	24	-52	35	9.48
Supramarginal gyrus	Right	40		36	-46	41	8.08
Supramarginal gyrus	Right	40		48	-31	50	7.48
Superior frontal gyrus	Left		79	-30	56	20	9.46
Frontopolar area	Left	10		-33	35	29	6.03
Cerebellum	Right		67	24	-64	-49	7.43

TABLE 1 (Continued)

Area	Hemisphere	BA	Cluster	MNI			t-value
				x	y	z	
Cerebellum	Right			18	-67	-43	6.66
Cerebellum	Right			33	-52	-52	6.35
Orbitofrontal area	Right	11	25	21	44	-16	7.22
Pre-motor and supplementary motor cortex	Left	6	23	-30	-7	68	6.64
Pre-motor and Supplementary motor cortex	Left	6	10	-24	-7	53	6.33
Expected reward >0							
Fusiform gyrus	Left	37	1091	-36	-49	-13	12.89
Fusiform gyrus	Left	37		-39	-64	-10	11.69
Visual association cortex	Left	19		-36	-73	-10	10.99
Visual association cortex	Right	19	1021	36	-76	-4	12.25
Fusiform gyrus	Right	37		39	-61	-13	11.69
Primary visual cortex	Right	17		18	-91	5	10.65
Parahippocampal gyrus	Right	30	19	18	-49	5	7.03
Unexpected loss >0							
Inferior prefrontal gyrus	Right	47	12,123	51	23	-4	15.18
Fusiform gyrus	Left	37		-33	-52	-16	14.95
Inferior prefrontal gyrus	Right	47		42	20	-7	14.22
Inferior prefrontal gyrus	Left	47	536	-33	17	-16	11.68
Insula	Left	13		-30	17	14	7.26
Cerebellum	Left		13	-9	-55	-40	6.72
Cerebellum	Right		16	12	-58	-40	6.66
Cerebellum	Right			3	-55	-40	5.91
Dorsal anterior cingulate cortex	Left	32	15	-27	41	14	6.58
0 > unexpected loss							
Pre-motor and supplementary motor cortex	Right	6	74	3	-22	65	8.26
Primary motor cortex	Right	4	41	33	-16	53	7.15
Reward anticipation > decision making							
Caudate	Left		12	-27	-43	8	6.87
Decision making > reward anticipation							
Somatosensory cortex	Left	3	16,737	-42	-22	44	18.27
Somatosensory cortex	Left	3		-45	-19	56	18.12
Primary motor cortex	Left	4		-36	-31	62	17.05
Frontopolar area	Left	10	211	-27	41	26	10.32
Dorsolateral prefrontal cortex	Left	9		-33	38	35	7.93
Cerebellum	Right		62	0	-25	-40	8.74
Expected reward > unexpected loss							
Pre-motor and supplementary motor cortex	Right	6	12	9	-19	62	6.49
Unexpected loss > expected reward							
Inferior prefrontal gyrus	Right	47	728	36	20	-19	14.45
Inferior prefrontal gyrus	Right	47		51	23	-4	12.06

(Continues)

TABLE 1 (Continued)

Area	Hemisphere	BA	Cluster	MNI			t-value
				x	y	z	
Inferior prefrontal gyrus	Right	47		42	17	-7	10.79
Inferior prefrontal gyrus	Left	47	402	-36	17	-19	12.03
Insula	Left	13		-36	14	2	7.28
Insula	Left	13		-33	20	8	7.04
Pre-motor and supplementary motor cortex	Right	6	1992	15	14	65	11.91
Dorsal anterior cingulate cortex	Right	32		9	38	26	11.62
Ventral anterior cingulate cortex	Left	24		-3	38	11	11.43
Supramarginal gyrus	Right	40	362	57	-46	35	8.73
Supramarginal gyrus	Right	40		57	-37	35	8.43
Middle Temporal gyrus	Right	21		48	-25	-7	7.91
Visual association cortex	Right	18	1251	21	-79	-10	8.38
Visual association cortex	Left	19		-27	-79	-16	7.88
Fusiform gyrus	Right	37		33	-46	-19	7.87
Ventral posterior cingulate cortex	Right	23	63	3	-16	32	7.72
Supramarginal gyrus	Left	40	79	-60	-52	26	7.42
Supramarginal gyrus	Left	40		-57	-49	38	7.37
Frontopolar area	Left	9	61	-24	47	29	6.88
Dorsolateral prefrontal cortex	Left	10		-24	41	20	6.76
Frontopolar area	Left			-30	50	14	6.24
Hypothalamus	Right		38	6	-4	-1	6.79
Caudate	Right			6	-1	14	6.14
Thalamus	Right			6	-10	20	6.11

Expected reward &gt; uncertain reward

n.s.

Uncertain reward &gt; expected reward

Pre-motor and supplementary motor cortex	Left	6	408	-6	5	53	10.46
Dorsal anterior cingulate cortex	Right	32		9	29	29	8.23
Dorsal anterior cingulate cortex	Left	32		-9	20	38	7.84
Somatosensory Cortex	Left	2	337	-42	-25	50	9.03
Pre-motor and supplementary motor cortex	Left	6		-27	-10	56	8.34
Pre-motor and supplementary motor cortex	Left	6		-30	-10	65	7.24
Cerebellum	Right		67	39	-46	-34	7.95
Cerebellum	Right			18	-52	-22	6.86
Dorsolateral prefrontal cortex	Right	9	148	33	38	32	7.95
Dorsolateral prefrontal cortex	Right	9		27	44	35	7.63
Frontopolar area	Right	10		33	53	26	7.63
Insula	Left	13	25	-36	14	5	7.63
Cerebellum	Left		18	-42	-52	-34	7.13
Frontopolar area	Left	10	19	-33	56	17	6.74
Dorsolateral prefrontal cortex	Left	9	34	-33	38	32	6.62
Frontopolar area	Left	10		-27	47	32	6.50

TABLE 1 (Continued)

Area	Hemisphere	BA	Cluster	MNI			<i>t</i> -value
				<i>x</i>	<i>y</i>	<i>z</i>	
Uncertain reward > unexpected loss							
n.s.							
Unexpected loss > uncertain reward							
Inferior prefrontal gyrus	Right	47	2627	33	17	-16	12.86
Inferior prefrontal gyrus	Right	47		51	23	-4	12.46
Fusiform gyrus	Right	37		27	-40	-16	11.09
Inferior prefrontal gyrus	Left	47	386	-33	17	-19	11.50
Middle temporal gyrus	Left	21		-39	-7	-16	7.57
Medial frontal gyrus	Right	8	1427	6	50	44	10.65
Dorsolateral prefrontal cortex	Right	9		3	53	20	10.50
Pre-motor and supplementary motor cortex	Right	6		9	20	65	10.25
Middle temporal gyrus	Right	21	565	51	-25	-7	9.15
Superior temporal gyrus	Right	22		57	-46	11	8.89
Primary and auditory association cortex	Right	42		57	-37	11	8.77
Ventral anterior cingulate cortex	Right	24	78	0	-16	38	8.77
Supramarginal gyrus	Left	40	195	-60	-52	26	8.72
Middle temporal gyrus	Left	21		-60	-49	8	6.63
Angular gyrus	Left	39		-54	-58	11	6.55
Midbrain	Right		24	3	-25	-22	7.58
Angular gyrus	Left	39	45	-42	-76	17	7.04
Visual association cortex	Left	19		-27	-88	11	6.77
Somatosensory association cortex	Right	7	132	12	-76	50	6.65
Somatosensory association cortex	Right	7		3	-79	35	6.43
Somatosensory association cortex	Right	7		12	-70	38	6.40
Thalamus	Right		12	6	-7	2	6.61
Thalamus	Left			-3	-10	2	5.94
Middle temporal gyrus	Left	21	11	-51	2	-28	6.52

hypotheses, unexpected loss prompted stronger activation in the bilateral insula and amygdala compared to null events.

Contrasts between the conditions show a small cluster of stronger activation in the caudate for reward anticipation than for decision making, and vice versa large clusters of stronger activation including insula, striatum, and mPFC for decision making compared to reward anticipation.

Expected rewards compared to unexpected losses have stronger activation in a small cluster in pre-motor cortex. The reverse contrast, unexpected losses minus expected rewards, has several large clusters of increased activation, including insula and mPFC reaching into ventral ACC and ventral PCC.

Expected rewards show no significantly stronger activation than uncertain rewards, but uncertain rewards are associated with increased activation compared to expected rewards in several clusters, including pre-motor cortex, dorsal ACC, DLPFC, insula, and frontopolar area.

Uncertain rewards show no increased activation compared to unexpected losses. But unexpected losses show stronger activation than uncertain rewards in widespread regions, including mPFC, insula, and ACC.

For all ROIs (Nacc, insula, ACC, amygdala, mPFC, DLPFC), activation was significantly stronger during decision making than during reward anticipation and also during unexpected losses than expected rewards. Uncertain rewards compared to expected rewards are

TABLE 2 Activation: small-volume correction.

Area	Hemisphere	Cluster	MNI			t-value
			x	y	z	
Decision making >0						
Nacc	Left	38	-12	11	-10	6.18
			-9	5	-10	6.04
Nacc	Right	44	15	5	-10	9.65
			15	14	-7	8.57
Insula	Left	572	-45	-1	5	12.53
			-42	-4	8	11.57
			-36	14	2	11.09
Insula	Right	343	36	23	5	11.45
			39	-1	11	9.83
			45	11	-4	9.79
ACC	Left	149	-6	23	26	9.51
ACC	Right	194	9	23	32	12.02
Amygdala	Left	18	-18	-4	-13	5.15
			-18	-10	-10	4.37
Amygdala	Right					n.s.
mPFC		153	-3	17	41	11.65
			6	20	41	9.44
			6	29	38	6.62
DLPFC	Left	82	-54	8	32	10.93
		61	-33	38	35	6.97
		10	-45	38	23	4.00
DLPFC	Right	365	45	5	38	10.92
			45	11	29	10.51
			54	8	35	10.22
Reward anticipation >0						
Nacc	Left	14	-9	5	-10	4.23
Nacc	Right	28	12	5	-10	5.84
			9	5	-4	4.43
Insula	Left	207	-33	23	8	10.29
			-30	23	-4	9.39
Insula	Right	148	33	26	-4	9.84
			33	26	5	9.43
			30	23	-10	9.14
ACC	Left					n.s.
ACC	Right					n.s.
Amygdala	Left					n.s.
Amygdala	Right					n.s.
mPFC		158	6	23	44	5.07
			6	32	41	4.83
DLPFC	Left	91	-45	5	35	5.83

TABLE 2 (Continued)

Area	Hemisphere	Cluster	MNI			t-value
			x	y	z	
DLPFC	Right	286	45	14	29	8.71
			48	29	17	7.86
			39	11	35	7.61
Uncertain reward >0						
Nacc	Left	48	-12	14	-7	7.80
			-9	5	-10	6.49
Nacc	Right	44	12	17	-7	8.06
			12	11	-7	7.98
			12	5	-10	7.86
Insula	Left	383	-39	17	-4	8.36
			-27	23	-10	7.68
			-27	23	11	7.43
Insula	Right	226	33	23	-10	10.00
			36	17	-1	7.98
			33	23	14	6.61
ACC	Left	161	-6	26	29	6.92
ACC	Right	187	9	23	32	9.44
Amygdala	Left	n.s.				
Amygdala	Right	26	15	-7	-13	4.02
			18	-1	-16	3.71
mPFC		338	6	20	41	8.63
			-9	29	29	5.33
			-12	35	26	4.54
DLPFC	Left	185	-42	5	38	6.30
			-36	38	35	5.74
			-42	32	35	5.29
DLPFC	Right	358	23	-45	35	4.25
			39	8	38	8.63
			45	29	23	8.63
			33	47	32	8.48
Expected reward >0						
Nacc	Left					n.s.
Nacc	Right					n.s.
Insula	Left					n.s.
Insula	Right					n.s.
ACC	Left					n.s.
ACC	Right					n.s.
Amygdala	Left					n.s.
Amygdala	Right					n.s.
mPFC						n.s.
DLPFC	Left					n.s.

(Continues)

TABLE 2 (Continued)

Area	Hemisphere	Cluster	MNI			t-value
			x	y	z	
DLPFC	Right	217	54	23	29	4.99
			42	11	35	4.78
			45	29	20	4.25
Unexpected loss >0						
Nacc	Left	33	-6	14	-10	3.43
			-6	20	-7	3.34
Nacc	Right	37	6	11	-4	3.35
			15	14	-13	3.26
Insula	Left	448	-33	17	-16	11.68
			-30	17	14	7.26
			-36	-7	-13	6.23
Insula	Right	345	42	20	-7	14.22
			33	17	-16	14.00
			42	-7	-13	4.81
ACC	Left	375	-9	32	20	11.38
			-3	38	8	9.99
			-3	23	17	9.56
ACC	Right	362	6	38	5	10.16
			6	38	11	10.11
			9	26	32	10.02
Amygdala	Left	84	-30	-4	-22	5.67
			-27	-1	-19	5.31
			-21	-13	-10	4.86
Amygdala	Right	91	24	-13	-13	6.55
			27	2	-22	6.46
			33	-4	-22	6.19
mPFC		1325	9	35	35	10.15
			6	26	59	9.37
			-3	38	32	9.33
DLPFC	Left	171	-24	50	35	4.57
			-54	20	29	4.36
			-42	8	38	4.28
DLPFC	Right	367	33	47	32	8.19
			48	29	17	7.97
			45	17	29	7.36
0 > unexpected loss						
Nacc	Left					n.s.
Nacc	Right					n.s.
Insula	Left					n.s.
Insula	Right					n.s.
ACC	Left					n.s.
ACC	Right					n.s.
Amygdala	Left					n.s.

TABLE 2 (Continued)

Area	Hemisphere	Cluster	MNI			t-value		
			x	y	z			
Amygdala	Right					n.s.		
mPFC						n.s.		
DLPFC	Left					n.s.		
DLPFC	Right					n.s.		
Reward anticipation > decision making								
Nacc	Left					n.s.		
Nacc	Right					n.s.		
Insula	Left					n.s.		
Insula	Right					n.s.		
ACC	Left					n.s.		
ACC	Right					n.s.		
Amygdala	Left					n.s.		
Amygdala	Right					n.s.		
mPFC						n.s.		
DLPFC	Left					n.s.		
DLPFC	Right					n.s.		
Decision making > reward anticipation								
Nacc	Left	41	-12	14	-7	6.53		
Nacc	Right	44	15	14	-7	9.62		
Insula	Left	588	-45	-1	5	13.79		
			-42	-4	8	12.89		
			-39	-7	11	12.84		
Insula	Right	468	45	5	2	11.76		
			39	-1	11	11.24		
			45	11	-4	10.85		
ACC	Left	318	-3	23	29	10.69		
			-9	44	-4	4.32		
ACC	Right	316	9	23	32	12.52		
			9	38	-7	4.34		
			6	44	-4	4.17		
Amygdala	Left	44	-18	-4	-13	5.01		
			-18	-10	-10	4.84		
			-30	-7	-28	4.11		
Amygdala	Right	27	33	-4	-25	3.17		
			mPFC	102	-3	17	41	13.39
					-9	29	29	6.36
mPFC		381	-9	26	35	6.31		
			6	53	-4	4.76		
			3	56	-7	4.74		
			9	50	-1	4.71		
DLPFC	Left	75	-54	8	32	11.06		
		74	-33	38	35	7.93		

(Continues)

TABLE 2 (Continued)

Area	Hemisphere	Cluster	MNI			t-value
			x	y	z	
DLPFC	Right	124	57	8	35	10.91
		100	30	38	35	7.59
			33	47	32	6.93
			30	32	35	6.89
Expected reward > unexpected loss						
Nacc	Left					n.s.
Nacc	Right					n.s.
Insula	Left					n.s.
Insula	Right					n.s.
ACC	Left					n.s.
ACC	Right					n.s.
Amygdala	Left					n.s.
Amygdala	Right					n.s.
mPFC						n.s.
DLPFC	Left					n.s.
DLPFC	Right					n.s.
Unexpected loss > expected reward						
Nacc	Left	30	-6	20	-7	4.06
Nacc	Right	362	0	38	11	10.68
			9	38	23	10.54
			6	35	8	10.14
Insula	Left	484	-33	17	-19	11.83
			-30	20	-13	10.78
			-36	14	2	7.28
Insula	Right	366	33	17	-16	12.66
			36	23	-19	12.36
			42	17	-7	10.79
ACC	Left	395	-3	38	11	11.43
			-6	38	26	10.83
			0	23	17	8.87
ACC	Right	362	0	38	11	10.68
			9	38	23	10.54
			6	35	8	10.14
Amygdala	Left	84	-30	-1	-25	5.15
			-18	-7	-13	5.12
			-27	-1	-19	5.07
Amygdala	Right	91	21	-4	-16	0.00
			27	2	-22	0.00
			24	-13	-13	0.00
mPFC		1373	-6	38	29	10.92
			0	50	20	9.74
			-9	41	20	9.19

TABLE 2 (Continued)

Area	Hemisphere	Cluster	MNI			t-value
			x	y	z	
DLPFC	Left	91	-27	47	35	6.20
			-33	26	35	4.83
DLPFC	Right	319	33	47	32	7.14
			39	29	44	4.92
			39	32	32	4.84
Expected reward > uncertain reward						
Nacc	Left					n.s.
Nacc	Right					n.s.
Insula	Left					n.s.
Insula	Right					n.s.
ACC	Left					n.s.
ACC	Right					n.s.
Amygdala	Left					n.s.
Amygdala	Right					n.s.
mPFC						n.s.
DLPFC	Left					n.s.
DLPFC	Right					n.s.
Uncertain reward > expected reward						
Nacc	Left	46	-12	11	-10	4.40286732
Nacc	Right	41	15	14	-7	4.80942822
Insula	Left	367	-36	14	5	7.63141441
			-33	20	-10	4.18157244
Insula	Right	248	33	23	-10	5.83683491
			42	14	2	5.60047531
			36	17	8	5.58169985
ACC	Left	205	-6	29	29	7.73474836
ACC	Right	41	15	14	-7	4.80942822
Amygdala	Left					n.s.
Amygdala	Right					n.s.
mPFC		331	0	29	32	7.29672146
			-6	32	29	7.04426432
			-3	17	41	6.72317123
DLPFC	Left	88	-27	47	35	6.40153313
DLPFC	Right	158	27	44	35	5.56693085
			39	32	32	4.77563148
Uncertain reward > unexpected loss						
Nacc	Left	15	-12	11	-10	3.21800017
Nacc	Right					n.s.
Insula	Left					n.s.
Insula	Right					n.s.
ACC	Left					n.s.
ACC	Right					n.s.
Amygdala	Left					n.s.

(Continues)

TABLE 2 (Continued)

Area	Hemisphere	Cluster	MNI			t-value
			x	y	z	
Amygdala	Right					n.s.
mPFC						n.s.
DLPFC	Left					n.s.
DLPFC	Right					n.s.
Unexpected loss > uncertain reward						
Nacc	Left					n.s.
Nacc	Right					n.s.
Insula	Left	362	-33	17	-19	11.5026321
			-36	-7	-13	6.35127878
			-39	-10	-7	5.11725044
Insula	Right	386	33	17	-16	12.8611927
			45	20	-7	9.9310236
			42	-7	-13	6.27829266
ACC	Left	397	0	23	17	9.2536974
			0	38	8	9.12949944
			-6	38	5	9.00330925
ACC	Right	362	6	44	8	10.022438
			6	38	5	9.98825836
			3	23	17	9.3745079
Amygdala	Left	84	-30	-4	-22	5.97138166
			-30	-10	-19	5.37122583
Amygdala	Right	91	24	-13	-13	6.8914156
			27	-1	-19	6.24873257
mPFC		1384	6	50	44	10.6491365
			3	53	20	10.4972439
			9	53	41	10.0991449
DLPFC	Left					n.s.
DLPFC	Right	188	54	32	14	5.02734947
			54	26	23	4.37021446
			45	17	29	4.25833178

associated with higher activation in all ROIs except amygdala. Expected compared to uncertain rewards had no stronger activation in any of the ROIs. Finally, uncertain rewards compared to unexpected losses had stronger activation in the left Nacc, but unexpected losses had stronger activation than uncertain rewards in all ROIs except Nacc and left DLPFC.

Whole-brain results of the parametric modulation of riskiness of decision show that riskier decisions are linked to stronger activation in the inferior prefrontal gyrus, caudate, hippocampus, and DLPFC (Figure 5). Small-volume correction confirmed stronger activation in the right insula with riskier decisions, but contrary to the hypothesis

no activation differences in the amygdala. Please refer to Table 3 for all whole-brain results from parametric modulation and Table 4 for all small-volume corrected results from parametric modulation.

Beyond that, exploratory ROI analyses revealed a negative association between riskiness during decision making and activation in bilateral Nacc, insula, amygdala, and left ACC. Whole-brain analyses for the same contrast, i.e., less riskiness during decision making, showed increased activation in widespread areas including insula, dorsal ACC, orbitofrontal area, DLPFC.

On a whole-brain level, reward anticipation during riskier trials was associated with increased activation in

several cortical regions including DLPFC and fusiform gyrus, whereas reward anticipation during lower-risk trials was associated with increased activation in areas including insula and dorsal ACC.

ROI analyses confirmed association of riskier trials with DLPFC, and lower-risk trials with Nacc, left Insula, and left ACC.

Exploratory whole-brain analyses revealed a positive association of higher-risk trials during uncertain reward feedback with DLPFC, Fusiform Gyrus, and further

visual processing areas. In contrast, lower-risk trials during uncertain reward feedback revealed stronger activation in insula, ventral PCC, and ventral ACC, as well as different areas associated with motor and visual processing.

ROI analyses showed increased activation in ACC, Amygdala, and mPFC for the positive association and increased activation in insula, ACC, mPFC, and DLPFC for the negative association.

### 3.3 | fMRI connectivity

Overall, left and right Nacc as seed regions showed connectivity to similar and overlapping cortical brain areas (Figure 5).

With increasing risk of the decisions, on a whole-brain level, there was increased connectivity to inferior prefrontal gyrus and frontopolar area reaching into ventral ACC.

ROI analyses confirmed increased connectivity with ACC, insula, and mPFC. Whole brain and small-volume corrected connectivity results are listed in Tables 5 and 6, respectively.

With increasing riskiness, whole-brain analyses showed increased connectivity to Fusiform Gyrus, inferior frontal and prefrontal gyrus reaching into insula, Hypothalamus, and areas of visual processing during the anticipation phase.

ROI analyses confirmed increased connectivity with right DLPFC and bilateral insula.

On a whole-brain level, with higher riskiness, uncertain rewards were associated with stronger connectivity to middle temporal gyrus, fusiform gyrus, DLPFC, and inferior frontal gyrus.

ROI analyses confirmed increased connectivity with bilateral DLPFC.

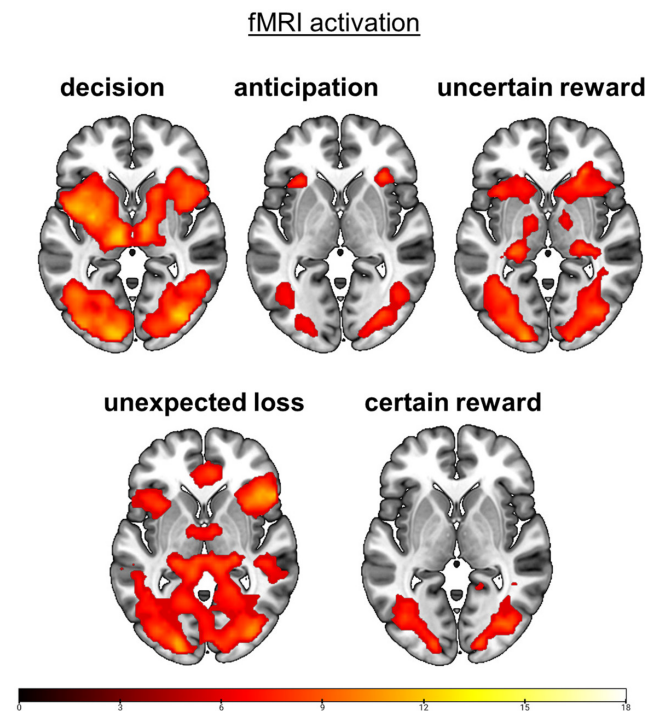
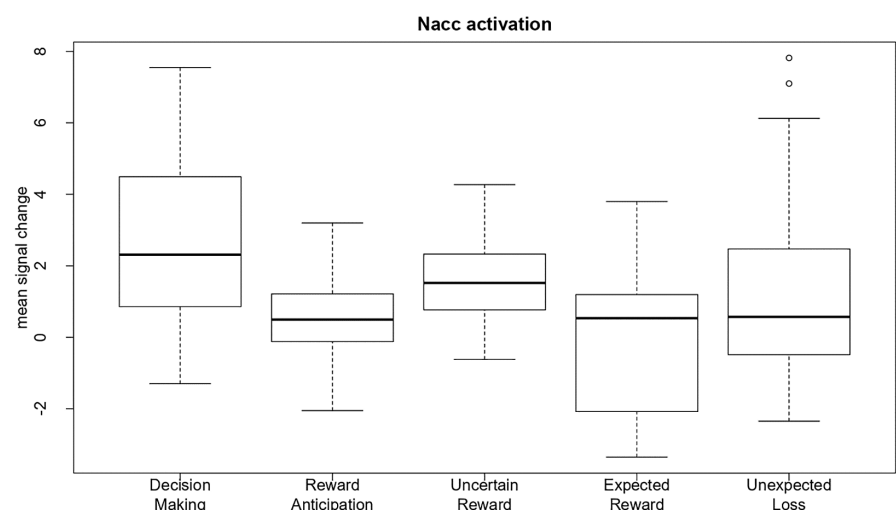
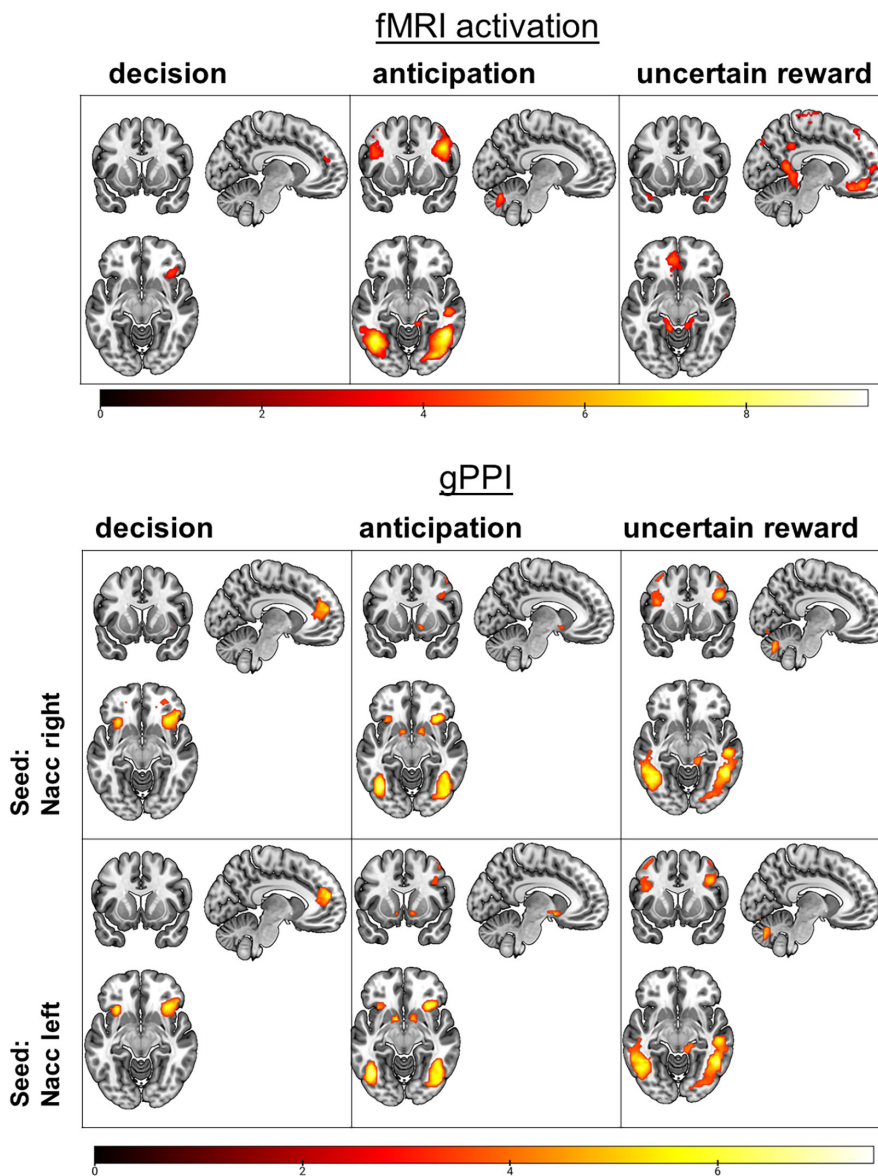


FIGURE 3 fMRI activation during all conditions versus the null events.  $p_{FWE} < .05$ , minimal cluster size  $k = 10$ . Bar to the bottom, indicating the  $T$ -values. Slice coordinate:  $Z = 0$ .

FIGURE 4 Boxplots depicting median, 25th and 75th percentile of the mean eigenvariate values over both Nacc-masks, with 1 value per participant per condition. Decision making, reward anticipation, and uncertain reward are significantly different to each other at  $p < .05$ . Expected reward and unexpected losses are only presented for completeness but are not subjected to statistical tests due to the low trial number and therefore low power.



## Decisions (pump) x parametric modulation of risk



**FIGURE 5** Parametric modulation of the distinct processes, activation, and gPPI connectivity results.  $p < .001$ , minimal cluster size  $k = 10$ . Colorbars indicating the  $T$ -values. Slice coordinates:  $X = -9$ ,  $Y = 10$ ,  $Z = -10$ .

## 4 | DISCUSSION

For the present study we developed a novel fMRI-variant of the widely used BART. The adapted BART not only preserves its original design but at the same time introduces three essential subprocesses of risk taking: decision making, reward anticipation and feedback. Our results show that the Nacc is differentially activated across all three subprocesses, further revealing functional connectivity to specific brain regions involved in decision making under varying levels of risk. This interaction, depending on the specific phase of the task and the level of risk involved, highlights the multifaceted nature of risky decision making which needs to be considered during the assessment. Overall, our results offer compelling evidence supporting

the assumption of differential functional activation and connectivity patterns throughout the course of risky decision making. This essential advancement emphasizes the instrumental value of our novel BART-variant.

While some of our findings align with our initial hypotheses based on existing literature, we also introduce highly relevant insights not reported previously. In agreement with our hypothesis, activation in Nacc was measured during decision making, reward anticipation, and uncertain reward feedback, but not during expected reward feedback. Contrary to our expectations, Nacc was also activated by unexpected loss feedback. Nacc activity upon uncertain, but lack of Nacc upon certain reward feedback (cash out condition) is in agreement with the role of the Nacc in motivational salience and uncertainty

**TABLE 3** Activation: Parametric modulation—whole brain.

Area	Hemisphere	BA	Cluster	MNI			t-value
				x	y	z	
Decision making × risk							
Positive correlation							
Caudate tail	Right		90	18	−34	20	5.69
Caudate tail	Right			24	−40	20	5.36
Inferior prefrontal gyrus	Right	47	144	42	23	2	5.57
Inferior prefrontal gyrus	Right	47		36	26	−10	4.46
Caudate tail	Left		71	−18	−37	17	5.02
Hippocampus	Left			−30	−49	5	4.13
Caudate tail	Left			−24	−46	11	4
Caudate body	Right		26	6	2	20	4.96
Frontopolar area	Right	10	37	18	50	26	4.38
Dorsolateral prefrontal cortex	Left	9	14	−9	44	23	4.13
Frontopolar area	Left	10		−9	50	17	4.02
Negative correlation							
Retrosplenial cingulate cortex	Right	29	7737	6	−46	14	8.54
Angular gyrus, part of Wernicke's area	Right	39		51	−61	23	7.79
Retrosplenial cingulate cortex	Left	29		−6	−40	8	7.15
Pre-motor and supplementary motor cortex	Left	6	86	−54	−4	11	5.46
Pars triangularis, part of Broca's area	Left	44		−48	−1	17	4.03
Insular cortex	Right	13	53	42	−34	20	5.1
Primary and auditory association cortex	Right	41		42	−43	11	3.85
Orbitofrontal area	Right	11	40	0	53	−16	4.56
Orbitofrontal area	Right	11		0	38	−16	4
Frontal eye field	Left	8	69	−24	11	47	4.56
Pre-motor and supplementary motor cortex	Left	6		−27	14	56	4.41
Pre-motor and supplementary motor cortex	Right	6	67	39	−10	35	4.37
Putamen	Right			33	−13	8	4.07
Insular cortex	Right	13		39	−13	14	3.7
Dorsal anterior cingulate cortex	Left	32	33	−6	11	38	4.04
Dorsal anterior cingulate cortex	Left	32		−9	11	47	3.85
Dorsolateral prefrontal cortex	Left	46	23	−48	35	17	3.99
Dorsolateral prefrontal cortex	Left	46		−39	29	17	3.73
Dorsolateral prefrontal cortex	Left	46		−45	35	26	3.65
Primary motor cortex	Left	4	13	−18	−31	71	3.91
Reward anticipation × risk							
Positive correlation							
Fusiform gyrus	Right	37	2208	45	−52	−13	9.46
Visual association cortex	Right	18		30	−82	2	8.06
Visual association cortex	Right	19		33	−79	−7	8.03

(Continues)

TABLE 3 (Continued)

Area	Hemisphere	BA	Cluster	MNI			<i>t</i> -value
				<i>x</i>	<i>y</i>	<i>z</i>	
Fusiform gyrus	Left	37	1179	-42	-58	-13	9.03
Fusiform gyrus	Left	37		-33	-49	-19	7.75
Visual association cortex	Left	19		-42	-70	-10	7.39
Dorsolateral prefrontal cortex	Right	9	582	45	11	32	7.81
Dorsolateral prefrontal cortex	Right	46		45	29	17	5.63
Pars opercularis Broca's area	Right	45		51	23	17	5.31
Supramarginal gyrus	Left	40	322	-33	-46	41	6.23
Visual association cortex	Left	19		-27	-73	32	4.97
Somatosensory association cortex	Left	7		-24	-58	44	4.85
Visual association cortex	Left	19	79	-30	-88	14	5.73
Visual association cortex	Left	19		-30	-82	8	5.07
Middle temporal gyrus	Right	21	66	51	-22	-13	5.67
Dorsolateral prefrontal cortex	Left	9	265	-42	11	26	4.98
Pre-motor and supplementary motor cortex	Left	6		-45	5	53	4.7
Insular cortex	Left	13		-33	17	26	4.59
Negative correlation							
Primary motor cortex	Left	4	877	-36	-22	59	8.77
Pre-motor and supplementary motor cortex	Left	6		-3	2	59	5.3
Dorsal anterior cingulate cortex	Left	32		-12	20	35	5.06
Insular cortex	Right	13	29	27	-43	20	5.11
Caudate tail	Right			18	-40	20	4.25
Insular cortex	Left	13	71	-45	-22	20	5.03
Insular cortex	Left	13		-42	-13	20	4.92
Insular cortex	Left	13	61	-48	5	8	4.91
Frontopolar area	Left	10	24	-27	38	20	4.34
Frontopolar area	Left	10		-30	35	29	4.31
Dorsal anterior cingulate cortex	Right	32	10	15	23	20	3.89
Caudate body	Right			21	20	14	3.82
Uncertain reward × risk							
Positive correlation							
Angular gyrus, part of Wernicke's area	Left	39	150	-42	-70	38	6.68
Angular gyrus, part of Wernicke's area	Left	39		-45	-67	29	6.04
Anterior entorhinal cortex	Right	34	96	18	-10	-22	6.6
Temporopolar area	Right	38		36	11	-31	4.58
Posterior entorhinal cortex	Right	28		30	5	-28	4.35
Cerebellum	Left		280	-15	-37	-16	6.47
Perirhinal cortex	Left	35		-21	-28	-16	5.96
Retrosplenial cingular cortex	Left	29		-6	-52	11	5.47
Subgenual cortex	Left	25	352	-6	29	-19	6.13
Frontopolar area	Left	10		-9	41	-13	6.09
Inferior prefrontal gyrus	Left	47		-15	32	-19	5.37

TABLE 3 (Continued)

Area	Hemisphere	BA	Cluster	MNI			t-value
				x	y	z	
Somatosensory association cortex	Right	7	162	3	-79	44	5.98
Somatosensory association cortex	Right	7		18	-79	44	5.25
Visual association cortex	Left	19		-9	-85	38	3.99
Primary motor cortex	Right	4	467	15	-25	71	5.8
Somatosensory cortex	Right	3		21	-34	71	5.78
Pre-motor and supplementary motor cortex	Right	6		6	-22	59	5.65
Cerebellum	Right		107	9	-40	-4	5.43
Perirhinal cortex	Right	35		18	-31	-13	4.74
Cerebellum	Right			9	-37	-16	4.27
Superior temporal gyrus	Right	22	76	63	-4	2	5.21
Superior temporal gyrus	Right	22		54	-7	5	4.92
Superior temporal gyrus	Right	22		60	2	-4	4.49
Includes frontal eye field	Left	8	72	-15	29	47	5.18
Dorsal posterior cingular cortex	Left	31	69	-6	-49	35	5.09
Temporopolar area	Left	38	54	-39	5	-22	4.92
Temporopolar area	Left	38		-33	5	-31	4.18
Temporopolar area	Left	38		-42	17	-22	4.14
Inferior Temporal gyrus	Left	20	12	-60	-13	-22	4.58
Primary and auditory association cortex	Left	42	16	-63	-31	17	4.02
Primary and auditory association cortex	Left	41		-54	-28	8	3.82
Negative correlation							
Pre-motor and supplementary motor cortex	Left	6	6006	-36	-10	59	11.24
Pre-motor and supplementary motor cortex	Left	6		-24	-7	56	11.15
Pre-motor and supplementary motor cortex	Left	6		-6	5	56	11.14
Somatosensory association cortex	Right	7	578	21	-55	41	10.6
Insular cortex	Right	13		48	-46	14	5.24
Insular cortex	Right	13		48	-37	23	5.23
Primary visual cortex	Left	17	597	-15	-88	-7	9.39
Visual association cortex	Left	18		-21	-82	-7	8.67
Fusiform gyrus	Left	37		-42	-52	-13	6.26
Cerebellum	Right		228	18	-52	-22	6.78
Cerebellum	Right			24	-49	-28	6.42
Cerebellum	Right			33	-43	-34	6.19
Primary visual cortex	Right	17	212	18	-91	5	6.59
Visual association cortex	Right	18		24	-88	17	4.86
Lingual gyrus	Right			33	-73	-4	4.45
Somatosensory cortex	Right	2	84	42	-28	44	6.27
Primary motor cortex	Right	4		54	-16	44	4.75

(Continues)

TABLE 3 (Continued)

Area	Hemisphere	BA	Cluster	MNI			<i>t</i> -value
				<i>x</i>	<i>y</i>	<i>z</i>	
Caudate	Right		49	12	−13	29	5.81
Ventral posterior cingulate cortex	Right	23		9	−28	26	4.42
Ventral anterior cingulate cortex	Right	24		18	−13	35	3.66
Cerebellum	Right		28	21	−58	−52	5.09
Cerebellum	Left		45	−9	−76	−37	5
Cerebellum	Left			−12	−76	−28	4.79
Cerebellum	Right		55	0	−58	−37	4.93
Cerebellum	Right			6	−64	−31	4.4
Insular cortex	Left	13	26	−39	−28	26	4.29
Insular cortex	Left	13		−48	−22	23	4.1
Cerebellum	Right		20	3	−31	−37	4.16
Cerebellum	Left		19	−33	−49	−31	4.09
Cerebellum	Left			−24	−52	−31	4.02
Frontopolar area	Left	10	39	−33	44	23	4.07
Frontopolar area	Left	10		−33	41	32	3.83

of rewards (Berridge, 2007; Cooper & Knutson, 2008; Matthews et al., 2004; Zink et al., 2004). Striatal activation upon risky decision making in the BART was reported before (Burnette et al., 2021; Li et al., 2020; Wang et al., 2022). A new finding, however, allowed by the present BART-variant, is the hierarchy of Nacc activation with strongest activation during the decision phase, medium activation during uncertain reward feedback, and weaker activation during reward anticipation. This suggests that the Nacc is involved in evaluating the potential risks and rewards of different options and thereby supports the choice of the most favorable option. In the BART, the risk of balloon popping and monetary loss is weighted against the chance of successful balloon inflation which signals monetary gain. This active decision making processes might be related to enhanced dopamine release, which is indicated by enhanced Nacc activity during decision making and processing of uncertain rewards.

We also find Nacc activity during the anticipation phase. This is in line with previous studies reporting increased ventral striatal activation for reward anticipation (Knutson, Adams, et al., 2001; Knutson & Greer, 2008; Rademacher et al., 2014). A new finding, though, is that anticipation prompted less Nacc activation than the decision and the feedback phase for uncertain rewards. This suggests that reward anticipation is a more passive process and does not involve the evaluation of potential risks and rewards for further decisions.

Stronger Nacc activation for the loss than the reward feedback replicates the findings by e.g., Rao et al. (2008). As loss feedback is not rewarding, Nacc activation upon

loss feedback might reflect salience and the evaluation of prospective decisions. Indeed, stronger Nacc activation for salience than for reward has also been suggested in a study on social decision making (Schmidt et al., 2019). Another explanation for Nacc activation upon loss feedback might be that sometimes participants were already expecting the explosion together with the associated monetary loss: Confirmation of a correct expectation might have been experienced as rewarding (Ruissen et al., 2018). Upon loss feedback, in addition to the amygdala, the insula was also activated, indicating that the insula is also involved in negative, aversive emotions and might also signal loss aversion or risk prediction error (Burnette et al., 2021; Li et al., 2020). Increased insula activation with less risky decisions might reflect increased strain to not lose the potential reward already at the beginning of the trial. The ACC activation that goes hand in hand with the insula activation in response to loss, may hint towards the proposed insula-ACC circuitry in loss aversion (Fukunaga et al., 2012; Xue et al., 2010).

In contrast to our expectations, high-risk decisions were associated with lower, not higher Nacc activation. Thus, present results contrast previous reports (Burnette et al., 2021; Claus & Hutchison, 2012). While activation in ACC, mPFC, amygdala, and insula was reduced, there was also a cluster with enhanced insula activity, Nacc connectivity with ACC, insula, and mPFC was increased. This suggests that the processing of different levels of risk is not simply related to changing intensity of involvement of a fixed set of structures, but different neural circuits seem involved. Thus, the stronger

TABLE 4 Activation: Parametric modulation – small volume correction.

Area	Hemisphere	Cluster	MNI			t-value
			x	y	z	
Decision making × risk						
Positive correlation						
Nacc	Left					n.s.
Nacc	Right					n.s.
Insula	Left					n.s.
<b>Insula</b>	<b>Right</b>	135	42	23	2	5.57
			36	23	−4	4.32
			39	26	−7	4.32
ACC	Left					n.s.
ACC	Right					n.s.
Amygdala	Left					n.s.
Amygdala	Right					n.s.
mPFC						n.s.
DLPFC	Left					n.s.
DLPFC	Right					n.s.
Negative correlation						
<b>Nacc</b>	<b>Left</b>	50	−6	11	−7	5.14
			−9	17	−7	4.98
			−12	14	−13	4.80
<b>Nacc</b>	<b>Right</b>	44	6	8	−10	4.83
			15	14	−13	3.62
<b>Insula</b>	<b>Left</b>	238	−39	−4	−13	5.57
			−36	−7	−7	4.92
<b>Insula</b>	<b>Right</b>	166	42	−7	−13	4.17
<b>ACC</b>	<b>Left</b>	81	−9	23	−13	3.95
ACC	Right					n.s.
<b>Amygdala</b>	<b>Left</b>	84	−15	−10	−13	5.36
<b>Amygdala</b>	<b>Right</b>	91	21	−4	−19	5.61
			30	−1	−22	5.00
			24	−4	−28	3.99
mPFC						n.s.
DLPFC	Left					n.s.
DLPFC	Right					n.s.
Reward anticipation × risk						
Positive correlation						
Nacc	Left					n.s.
Nacc	Right					n.s.
Insula	Left					n.s.
Insula	Right					n.s.
ACC	Left					n.s.
ACC	Right					n.s.
Amygdala	Left					n.s.
Amygdala	Right					n.s.

(Continues)

TABLE 4 (Continued)

Area	Hemisphere	Cluster	MNI			<i>t</i> -value
			<i>x</i>	<i>y</i>	<i>z</i>	
mPFC						n.s.
<b>DLPFC</b>	<b>Left</b>	73	-54	20	29	4.54
			-48	14	29	4.51
			-45	11	35	4.43
		31	-51	29	17	4.51
<b>DLPFC</b>	<b>Right</b>	240	45	11	32	7.81
			51	20	26	6.63
			48	29	20	5.25
Negative correlation						
<b>Nacc</b>	<b>Left</b>	33	-12	11	-10	3.57
<b>Nacc</b>	<b>Right</b>	27	9	17	-7	3.77
			12	14	-10	3.18
<b>Insula</b>	<b>Left</b>	267	-42	5	5	4.79
			-42	2	11	4.38
			-39	-13	20	4.31
Insula	Right					n.s.
<b>ACC</b>	<b>Left</b>	144	-6	23	32	4.20
ACC	Right					n.s.
Amygdala	Left					n.s.
Amygdala	Right					n.s.
mPFC						n.s.
DLPFC	Left					n.s.
DLPFC	Right					n.s.
Uncertain reward × risk						
Positive correlation						
Nacc	Left					n.s.
Nacc	Right					n.s.
Insula	Left					n.s.
Insula	Right					n.s.
<b>ACC</b>	<b>Left</b>	148	-6	29	-13	5.77
			-6	35	-16	5.72
			-3	41	-13	5.58
<b>ACC</b>	<b>Right</b>	56	0	32	-13	4.97
			6	29	-13	4.67
<b>Amygdala</b>	<b>Left</b>	36	-21	-13	-19	4.50
<b>Amygdala</b>	<b>Right</b>	62	21	-10	-19	6.47
			27	2	-28	3.71
<b>mPFC</b>		614	-9	41	-13	6.09
			-6	29	-13	5.77
			-3	41	-13	5.58
DLPFC	Left					n.s.
DLPFC	Right					n.s.
Negative correlation						

TABLE 4 (Continued)

Area	Hemisphere	Cluster	MNI			t-value
			x	y	z	
Nacc	Left					n.s.
Nacc	Right					n.s.
<b>Insula</b>	<b>Left</b>	383	-27	23	-7	8.75815964
			-33	17	8	8.11680031
			-27	20	2	6.86326361
<b>Insula</b>	<b>Right</b>	250	36	20	8	9.36728764
			33	26	-1	7.70193529
			30	23	-10	7.6050415
<b>ACC</b>	<b>Left</b>	78	-9	23	26	5.35270929
<b>ACC</b>	<b>Right</b>	109	12	26	26	6.36187553
			9	23	29	6.16349936
Amygdala	Left					n.s.
Amygdala	Right					n.s.
<b>mPFC</b>		166	6	20	41	5.70552683
			-9	17	41	5.52102566
<b>DLPFC</b>	<b>Left</b>	91	-57	8	29	7.42971039
			-48	2	32	5.1486764
			-42	5	38	4.96873617
<b>DLPFC</b>	<b>Right</b>	355	45	11	29	8.98030376
			54	11	32	7.14651823
			42	5	35	7.13101912

Nacc-connectivity with the higher-risk decision might reflect the increased cognitive and emotional demands of making decisions that involve greater potential risks. Participants may have felt confident and certain in the lower-risk decisions, so there was no need to control or down-regulate the limbic response. Moreover, the rewarding potential was not yet large. Another possible explanation might be a differential role of the Nacc dependent on the riskiness. For lower-risk decisions, the Nacc might be more involved in the processing of reward, whereas in the case of higher-risk decisions, it might be more involved in risk and uncertainty processing, as indicated by the connectivity patterns with insula and ACC. Importantly, Nacc-ACC connectivity increased with higher risk, only in the decision phase. Based on the known associations of brain regions and functional involvement, one would at first glance expect higher activation of all regions for higher-risk inflations. However, pump decisions early in the trial (low risk) will differ from strategies later in the series of inflations. Risk assessment for small balloons and early inflations might reflect one's own willingness to take a risk for the current balloon, involving the insula, and develop an according strategy by integrating emotions and thoughts

via ACC. Importantly, with increasing risk, the Nacc-ACC-insula monitoring network of riskiness seems to be only increasingly involved during the decisions, suggesting that the process is temporally bound to this early phase and does not proceed to anticipation and feedback processing.

Reward anticipation and uncertain reward feedback were characterized by common and also distinct patterns of connectivity. In the anticipation phase, Nacc, insula, and ACC activation were decreased with increasing risk, but activity in another insula cluster, as well as in DLPFC enhanced, and also Nacc-DLPFC-connectivity increased. For uncertain reward feedback, activation in ACC, amygdala, and mPFC was enhanced, and in insula ACC, DLPFC, and another mPFC cluster reduced. Nacc-DLPFC connectivity increased with increasing risk. As one interpretation, we suggest that the enhanced Nacc-insula connectivity with increasing risk during anticipation reflects participants contemplating more on their own values, goals, and strategies. The increased connectivity of Nacc and inferior frontal gyrus during anticipation after high-risk decisions might be associated with the increased regulation of behavior towards unexpected events and the ensuing ability to adjust the behavior accordingly. Moreover, stronger

TABLE 5 Connectivity gPPI: Whole brain.

Area	Hemisphere	BA	Cluster	MNI			t-value
				x	y	z	
Decision making × risk							
Seed: Nacc left							
Inferior prefrontal gyrus	Right	47	397	42	23	2	6.68
Inferior prefrontal gyrus	Right	47		36	26	-10	6.23
Inferior prefrontal gyrus	Right	47		45	32	-7	5.52
Frontopolar area	Left	10	567	-9	50	17	6.44
Dorsolateral prefrontal cortex	Left	9		-9	44	23	5.65
Ventral anterior cingulate cortex	Right	24		9	38	-1	5.57
Inferior prefrontal gyrus	Left	47	108	-30	23	-10	6.2
Inferior prefrontal gyrus	Left	47		-39	23	-4	4.39
Caudate tail	Right		11	21	-34	17	3.97
Supramarginal gyrus	Right	40	18	54	-43	32	3.95
Caudate body	Right		13	6	5	17	3.92
Seed: Nacc right							
Inferior prefrontal gyrus	Right	47	1345	42	23	2	7.03
Inferior prefrontal gyrus	Right	47		33	20	-13	6.29
Inferior prefrontal gyrus	Right	47		39	29	-4	5.93
Inferior prefrontal gyrus	Left	47	109	-30	23	-10	5.59
Inferior prefrontal gyrus	Left	47		-39	23	-4	4.3
Supramarginal gyrus	Right	40	38	54	-40	35	4.64
Caudate body	Right		21	6	5	14	3.99
Reward anticipation × risk							
Seed: Nacc left							
Visual association cortex	Left	19	535	-42	-70	-13	7.25
Visual association cortex	Left	18		-33	-85	-1	5.9
Fusiform gyrus	Left	37		-42	-49	-19	5.81
Fusiform gyrus	Right	37	628	45	-58	-13	7
Visual association cortex	Right	19		33	-91	5	6.95
Fusiform gyrus	Right	37		42	-49	-10	6.29
Pars opercularis Broca's area	Right	45	410	33	26	5	6.84
Inferior prefrontal gyrus	Right	47		30	23	-7	6.84
Insular cortex	Right	13		42	23	11	5.9
	Left		71	-9	5	-10	6.18
Medial globus pallidus	Right			12	2	-7	5.53
Hypothalamus	Left			-3	-1	-7	5.16
Inferior prefrontal gyrus	Left	47	91	-30	23	-7	5.44
Insular cortex	Left	13		-39	23	8	4.78
Somatosensory association cortex	Right	7	65	24	-52	41	4.51
Pre-motor and supplementary motor cortex	Right	6	17	6	32	41	3.95
Middle temporal gyrus	Right	21	10	51	-28	-4	3.83
Seed: Nacc right							
Pars opercularis Broca's area	Right	45	364	33	26	5	7.29

TABLE 5 (Continued)

Area	Hemisphere	BA	Cluster	MNI			t-value
				x	y	z	
Inferior prefrontal gyrus	Right	47		30	23	-7	6.86
Insular cortex	Right	13		42	23	11	6.04
Visual association cortex	Right	19	585	33	-91	5	7.06
Fusiform gyrus	Right	37		45	-58	-13	6.7
Visual association cortex	Right	19		39	-70	-16	6.11
Visual association cortex	Left	19	502	-42	-70	-13	6.97
Fusiform gyrus	Left	37		-42	-61	-10	6.64
Visual association cortex	Left	18		-33	-85	-1	5.94
Lateral globus pallidus	Right		36	12	5	-7	5.83
Inferior prefrontal gyrus	Left	47	85	-30	23	-7	5.54
Insular cortex	Left	13		-39	23	8	4.53
Medial globus pallidus	Left		21	-12	2	-7	5.05
Hypothalamus	Left			-3	-1	-7	4.03
Somatosensory association cortex	Right	7	61	24	-52	41	4.74
Angular gyrus	Right	39	20	45	-52	8	4.32
Dorsolateral prefrontal cortex	Right	9	20	9	32	38	4.06
Uncertain reward × risk							
Seed: Nacc left							
Fusiform gyrus	Right	37	1579	48	-49	-13	7.34
Cerebellum	Right			12	-79	-31	6.36
Middle temporal gyrus	Right	21		51	-22	-13	6.21
Cerebellum	Left		1103	-21	-70	-43	7.31
Visual association cortex	Left	19		-48	-58	-13	6.81
Cerebellum	Left			-12	-76	-37	6.29
Right cerebrum	Right	27	86	12	-34	-4	6.89
Pars opercularis Broca's area	Right	45	379	51	23	26	5.77
Dorsolateral prefrontal cortex	Right	9		42	11	35	5.24
Dorsolateral prefrontal cortex	Right	46		51	29	17	5.21
Somatosensory association cortex	Left	7	274	-33	-61	41	5.4
Somatosensory association cortex	Left	7		-30	-49	41	4.75
Dorsolateral prefrontal cortex	Left	46	365	-54	29	14	5.37
Dorsolateral prefrontal cortex	Left	46		-42	14	26	5.06
Inferior prefrontal gyrus	Left	47		-51	35	-4	5
Orbitofrontal area	Right	11	13	18	47	-16	4.39
Pre-motor and supplementary motor cortex	Left	6	33	-42	5	53	4.23
Pre-motor and supplementary motor cortex	Left	6		-36	11	59	4.11
Seed: Nacc right							
Fusiform gyrus	Right	37	1570	48	-49	-13	7.29
Middle temporal gyrus	Right	21		51	-22	-13	6.78
Cerebellum	Right			12	-79	-31	6.59
Cerebellum	Left		1092	-21	-70	-43	7.28

(Continues)

TABLE 5 (Continued)

Area	Hemisphere	BA	Cluster	MNI			<i>t</i> -value
				<i>x</i>	<i>y</i>	<i>z</i>	
Visual association cortex	Left	19		-48	-58	-13	7
Cerebellum	Left			-12	-76	-37	6.62
Right cerebrum	Right	27	81	12	-34	-4	6.83
Somatosensory association cortex	Left	7	309	-33	-61	41	5.8
Supramarginal gyrus	Left	40		-33	-46	41	5.11
Somatosensory association cortex	Left	7		-27	-52	38	4.9
Pars opercularis Broca's area	Right	45	401	51	23	26	5.65
Dorsolateral prefrontal cortex	Right	9		42	11	35	5.31
Dorsolateral prefrontal cortex	Right	46		51	32	17	5.17
Dorsolateral prefrontal cortex	Left	46	383	-54	29	14	5.46
Dorsolateral prefrontal cortex	Left	46		-42	14	26	5.21
Inferior prefrontal gyrus	Left	47		-48	32	-4	5.1
Orbitofrontal area	Right	11	14	18	47	-16	4.33
Pre-motor and supplementary motor cortex	Left	6	29	-42	5	53	4.14
Pre-motor and supplementary motor cortex	Left	6		-33	17	59	3.76

inferior frontal gyrus (and insula) activation for riskier trials has been associated with loss aversion (Fukunaga et al., 2012). Similarly, reward anticipation and uncertain reward feedback under higher risk were both characterized by stronger connectivity between Nacc and DLPFC. During anticipation, this connectivity was lateralized from both Nacc seeds to only the right DLPFC, whereas in response to reward feedback, connectivity between Nacc and bilateral DLPFC predominated. Given that knowledge on distinct DLPFC-connectivity patterns is still limited (Cipolotti et al., 2016; Kaller et al., 2011), we can only assume that processing reward feedback in comparison to the anticipation of a reward requires additional cognitive resources, as it may involve the integration of previous experience and adjustment of future decision strategies. These enhanced cognitive demands might then be reflected by bilateral instead of just unilateral activation. In addition, for later feedback, activation of DLPFC might reflect greater demands on working memory capacity to keep count of the number of inflations or expected rewards, and also by the increased uncertainty. Importantly, it is to be expected that at the time of the feedback, the brain already starts weighing the risks against the benefits and preparing for the upcoming decision, so these processes might be included in the feedback phase and visible in the neural activation patterns.

The response times to cash-out decisions were the fastest, followed by inflation decisions that led to uncertain rewards, and inflation decisions leading to unexpected

losses were the slowest. Given that cash-out decisions carry no risk and are the fastest, one could speculate that these no-risk decisions are related to less hesitation. In contrary, participants may have been aware of a high risk of explosion in those decision that led to unexpected losses, and this process of gambling and overcoming the fear of loss led to the longer reaction times.

Some shortcomings of the present study should be noticed. Several regions were implicated in opposing contrasts, such as the insula. However, riskier decisions were associated with activation in more anterior parts of the insula, while lower-risk decision activations were located more posterior. To our knowledge, only one meta-analysis so far has evaluated the functional differentiation of the insula for different tasks (Kurth et al., 2010). Further studies are needed to evaluate the implications of different insular locations for risky decision making. The number of 12 balloons that could be inflated a maximum 8 times considered the participants' attention capacity during fMRI monitoring, yet may be insufficient for averaging and, hence, robust results. As a step towards verifying reliability and robustness of the results, behavioral, activation, connectivity, and behavioral data were submitted to test-retest analyzes (which will be published separately). This reliability test will also provide the basis for longitudinal studies, intervention studies, and comparisons between different participant groups (e.g., clinical populations). A limited number of trials also limits the possibility to analyze the influence of unexpected loss experiences on risk

TABLE 6 Connectivity gPPI: Small volume correction.

Area	Hemisphere	Cluster	MNI			t-value
			x	y	z	
Decision making × risk						
Seed: Nacc left						
ACC	Left	211	-12	44	8	4.98
			-9	41	17	4.63
			-9	47	11	4.61
ACC	Right	263	9	38	-1	5.57
			0	29	11	4.05
DLPFC	Left					n.s.
DLPFC	Right					n.s.
mPFC		649	-9	50	17	6.44
			-9	44	23	5.65
			-3	47	26	5.19
Insula	Left	183	-30	23	-10	6.20
			-39	20	-1	4.15
Insula	right	193	42	23	2	6.68
			33	20	-13	6.04
			36	26	-7	5.84
Amygdala	Left					n.s.
Amygdala	Right					n.s.
Seed: Nacc right						
ACC	Left	225	-12	44	8	5.17
			-6	41	23	4.90
			-9	41	17	4.78
ACC	Right	275	9	38	-1	5.82
			12	41	5	4.33
			0	29	11	4.33
DLPFC	Left					n.s.
DLPFC	Right					n.s.
mPFC		722	-9	50	17	5.74
			-9	44	23	5.53
			-12	47	20	5.41
Insula	Left	185	-30	23	-10	5.59
			-39	20	-1	4.08
Insula	Right	199	42	23	2	7.03
			33	20	-13	6.29
			39	26	-7	5.82
Amygdala	Left					n.s.
Amygdala	Right					n.s.
Decision making × risk negative						
Seed: Nacc left						
ACC	Left					n.s.
ACC	Right					n.s.
DLPFC	Left					n.s.

(Continues)

TABLE 6 (Continued)

Area	Hemisphere	Cluster	MNI			t-value
			x	y	z	
DLPFC	Right					n.s.
mPFC						n.s.
Insula	Left					n.s.
Insula	Right					n.s.
<b>Amygdala</b>	<b>Left</b>	78	-21	-13	-13	4.16
			-18	-7	-22	3.56
			-24	-1	-25	3.43
<b>Amygdala</b>	<b>Right</b>	81	18	-4	-19	3.54
Seed: Nacc right						
ACC	Left					n.s.
ACC	Right					n.s.
DLPFC	Left					n.s.
DLPFC	Right					n.s.
mPFC						n.s.
Insula	Left					n.s.
Insula	Right					n.s.
<b>Amygdala</b>	<b>Left</b>	78	-21	-13	-13	4.44
			-24	-1	-25	3.44
			-18	-7	-22	3.43
<b>Amygdala</b>	<b>Right</b>	77	18	-4	-19	3.86
Reward anticipation × risk						
Seed: Nacc left						
ACC	Left					n.s.
ACC	Right					n.s.
DLPFC	Left					n.s.
<b>DLPFC</b>	<b>Right</b>	206	45	32	20	4.49
mPFC						n.s.
<b>Insula</b>	<b>Left</b>	117	-30	23	-7	5.44
			-33	26	-1	5.13
			-36	20	-7	5.02
<b>Insula</b>	<b>Right</b>	119	33	26	5	6.84
			36	23	-7	6.55
			30	23	-10	6.53
Amygdala	Left					n.s.
Amygdala	Right					n.s.
Seed: Nacc right						
ACC	Left					n.s.
ACC	Right					n.s.
DLPFC	Left					n.s.
<b>DLPFC</b>	<b>Right</b>	26	45	29	20	4.26
mPFC						n.s.

TABLE 6 (Continued)

Area	Hemisphere	Cluster	MNI			t-value	
			x	y	z		
<b>Insula</b>	<b>Left</b>	57	-30	23	-7	5.54	
			-33	26	-1	5.12	
			-36	20	-7	5.05	
<b>Insula</b>	<b>Right</b>	73	33	26	5	7.29	
			36	23	-7	6.50	
			30	23	-10	6.47	
Amygdala	Left				n.s.		
Amygdala	Right				n.s.		
Uncertain reward × risk							
Seed: Nacc left							
ACC	Left					n.s.	
ACC	Right					n.s.	
<b>DLPFC</b>	<b>Left</b>	31	-54	29	14	5.37	
			74	-54	20	29	4.86
			-48	17	32	4.68	
<b>DLPFC</b>	<b>Right</b>	217	51	23	26	5.77	
			42	11	35	5.24	
			51	29	17	5.21	
mPFC						n.s.	
Insula	Left					n.s.	
Insula	Right					n.s.	
Amygdala	Left					n.s.	
Amygdala	Right					n.s.	
Seed: Nacc right							
ACC	Left					n.s.	
ACC	Right					n.s.	
<b>DLPFC</b>	<b>Left</b>	31	-54	29	14	5.46	
			76	-54	20	29	4.92
			-48	17	32	4.73	
<b>DLPFC</b>	<b>Right</b>	218	51	23	26	5.65	
			42	11	35	5.31	
			51	32	17	5.17	
mPFC						n.s.	
Insula	Left					n.s.	
Insula	Right					n.s.	
Amygdala	Left					n.s.	
Amygdala	Right					n.s.	

behavior in the subsequent trial(s). Also, with regard to the parametric modulation, it would have been advantageous if the participants had seen more balloons per trial to increase the explanatory power.

One challenge of our task design is the fixed order of decision making, anticipation, and feedback processing,

because these are functionally interrelated subprocesses of decisions, causing the necessity of a consistent temporal order. Even if comparable fixed-order designs have been used in other decision making studies that aimed to separate subprocesses (Ernst et al., 2004; Fukunaga et al., 2012), this kind of design does not allow for strict

functional separation of activation patterns between the subprocesses, because later subtrials may contain functional components from the preceding subtrials.

As summarized by Ruge et al. (2009), there are two approaches to address this issue. The first approach involves using variable intervals between stimuli, which we have implemented in our task. In general, analogous to rapid event related designs, applying jittered interstimulus intervals (Dale, 1999) is considered to allow the distinction of events, also in multi-part trial designs. However, these still leave a risk that brain activation from earlier phases might be partly present in subsequent phases, and also does not solve the problem of the functional interrelatedness of the subprocesses. The second approach is the use of partial-trial designs, as also suggested by Ollinger et al. (2001). This method involves omitting some subtrials in a subset of blocks. However, the original partial-trial design has drawbacks, such as potential inhibition of activation when an expected subprocess is omitted. Ruge et al. (2009) proposed an extended version of the partial-trial design that mitigates core issues of the standard partial-trial method. Specifically, they used three different trial types: trials consisting of two events with a short ITI, trials consisting of two events with a longer ITI, and trials in which the second event was omitted. As an advancement to other partial-trial designs, their approach allows distinguishing (1) the transient activation related to the first stimulus, (2) the maintained activation related to the first stimulus, and (3) activation caused by omission of the second stimulus. Implementing such an extended partial-trial design in future research could significantly enhance our ability to separate the subprocesses of the BART task.

It would also be valuable to have a higher-level control condition instead of the null events. In particular, because the decision phase was the only condition that involved motor responses. Ideally, the control condition would be identical to the experimental condition but without monetary consequences. Since these control conditions, however, would have doubled the experimental time, it was not possible to realize this more elegant control design within the present study.

Another limitation arises from the strict inclusion criteria for mental health applied to study participants, which restricts the generalizability of our findings to a broader population. Individual risk-taking strategies and/or personality factors might modulate risk preferences (Oba et al., 2021) and thus brain activity and connectivity patterns. For instance, harm avoidance or neuroticism was related to insula activation during risky decisions (Paulus et al., 2003). This issue should be addressed in future studies with larger, diverse samples. Risky decision making and altered brain activity might also be influenced by acute stress through increased levels of cortisol (Yamakawa

et al., 2016), which participants might experience in varying degrees while MRI-measurement. The interaction of stress hormone release, altered decision making, and brain activity in the BART could be considered in future studies.

To conclude, the novel BART-variant for fMRI has proven its efficacy in the differentiation of brain activation and connectivity of the three functional and temporally interrelated subprocesses of risk taking. Each subprocess showed unique activation and connectivity patterns, varying in response to the degree of risk involved. This underscores the need for a nuanced exploration of diverse brain regions and neural networks in the assessment of risky decision making and strongly emphasizes the significance of assessing decision making, anticipation, and feedback processing. This novel BART-variant is promising for unraveling the intricacies of risky decision making, particularly in high-risk populations known to exhibit impairments in decision making and reward anticipation.

## AUTHOR CONTRIBUTIONS

**Stephanie N. L. Schmidt:** Data curation; formal analysis; investigation; software; visualization; writing – original draft; writing – review and editing. **Sarah Sehrig:** Writing – original draft; writing – review and editing. **Alexander Wolber:** Investigation; project administration; writing – review and editing. **Brigitte Rockstroh:** Conceptualization; funding acquisition; supervision; writing – review and editing. **Daniela Mier:** Conceptualization; funding acquisition; methodology; supervision; writing – review and editing.

## ACKNOWLEDGMENTS

This study was part of a DFG-funded project GZ: MI 1975/7-1. The authors thank our colleagues for their help in data collection and curation: Sarah Tholl, Alexander Sahm, Peter Diedrich. Also, many thanks to our participants in the study. Open Access funding enabled and organized by Projekt DEAL.

## CONFLICT OF INTEREST STATEMENT

None.

## DATA AVAILABILITY STATEMENT

The masks, as well as the BART presentation file and analysis scripts are available on <https://osf.io/pkbt6/>. In addition, we make the fMRI data (raw, converted nifit-files of the EPis) available upon request to researchers signing a data protection statement.

## ORCID

Stephanie N. L. Schmidt  <https://orcid.org/0000-0003-1579-5881>

Daniela Mier  <https://orcid.org/0000-0003-2518-7492>

## REFERENCES

- Alexander, W. H., & Brown, J. W. (2010). Computational models of performance monitoring and cognitive control. *Topics in Cognitive Science*, 2(4), 658–677.
- Bakker, R., Tiesinga, P., & Kötter, R. (2015). The scalable brain atlas: Instant web-based access to public brain atlases and related content. *Neuroinformatics*, 13(3), 353–366. <https://doi.org/10.1007/s12021-014-9258-x>
- Bechara, A., Dolan, S., Denburg, N., Hindes, A., Anderson, S. W., & Nathan, P. E. (2001). Decision-making deficits, linked to a dysfunctional ventromedial prefrontal cortex, revealed in alcohol and stimulant abusers. *Neuropsychologia*, 39(4), 376–389. [https://doi.org/10.1016/S0028-3932\(00\)00136-6](https://doi.org/10.1016/S0028-3932(00)00136-6)
- Becker, A., Kirsch, M., Gerchen, M. F., Kiefer, F., & Kirsch, P. (2017). Striatal activation and frontostriatal connectivity during non-drug reward anticipation in alcohol dependence. *Addiction Biology*, 22(3), 833–843.
- Beesdo-Baum, K., Zaudig, M., & Wittchen, H.-U. (2019). *SCID-5-CV Strukturiertes Klinisches Interview für DSM-5-Störungen—Klinische Version: Deutsche Bearbeitung des Structured Clinical Interview for DSM-5 Disorders—Clinician Version von Michael B. First, Janet B.W. Williams, Rhonda S. Karg, Robert L. Spitzer*. Hogrefe.
- Berridge, K. C. (2007). The debate over dopamine's role in reward: The case for incentive salience. *Psychopharmacology*, 191, 391–431.
- Bogg, T., Fukunaga, R., Finn, P. R., & Brown, J. W. (2012). Cognitive control links alcohol use, trait disinhibition, and reduced cognitive capacity: Evidence for medial prefrontal cortex dysregulation during reward-seeking behavior. *Drug and Alcohol Dependence*, 122, 112–118.
- Bornoalova, M. A., Daughters, S. B., Hernandez, G. D., Richards, J. B., & Lejuez, C. (2005). Differences in impulsivity and risk-taking propensity between primary users of crack cocaine and primary users of heroin in a residential substance-use program. *Experimental and Clinical Psychopharmacology*, 13(4), 311.
- Brown, J. W., & Braver, T. S. (2007). Risk prediction and aversion by anterior cingulate cortex. *Cognitive, Affective, & Behavioral Neuroscience*, 7(4), 266–277.
- Burnette, E. M., Grodin, E. N., Ghahremani, D. G., Galvan, A., Kohno, M., Ray, L. A., & London, E. D. (2021). Diminished cortical response to risk and loss during risky decision making in alcohol use disorder. *Drug and Alcohol Dependence*, 218, 108391.
- Burton, A. C., Bissonette, G. B., Vazquez, D., Blume, E. M., Donnelly, M., Heatley, K. C., Hinduja, A., & Roesch, M. R. (2018). Previous cocaine self-administration disrupts reward expectancy encoding in ventral striatum. *Neuropsychopharmacology*, 43(12), 2350–2360.
- Burton, A. C., Nakamura, K., & Roesch, M. R. (2015). From ventral-medial to dorsal-lateral striatum: Neural correlates of reward-guided decision-making. *Neurobiology of Learning and Memory*, 117, 51–59.
- Cipolotti, L., Spano, B., Healy, C., Tudor-Sfetea, C., Chan, E., White, M., Biondo, F., Duncan, J., Shallice, T., & Bozzali, M. (2016). Inhibition processes are dissociable and lateralized in human prefrontal cortex. *Neuropsychologia*, 93, 1–12. <https://doi.org/10.1016/j.neuropsychologia.2016.09.018>
- Claus, E. D., & Hutchison, K. E. (2012). Neural mechanisms of risk taking and relationships with hazardous drinking. *Alcoholism: Clinical and Experimental Research*, 36(6), 932–940.
- Cooper, J. C., & Knutson, B. (2008). Valence and salience contribute to nucleus accumbens activation. *NeuroImage*, 39(1), 538–547.
- Dale, A. M. (1999). Optimal experimental design for event-related fMRI. *Human Brain Mapping*, 8(2–3), 109–114. [https://doi.org/10.1002/\(Sici\)1097-0193\(1999\)8:2/3<109::Aid-Hbm7>3.0.Co;2-W](https://doi.org/10.1002/(Sici)1097-0193(1999)8:2/3<109::Aid-Hbm7>3.0.Co;2-W)
- Dolcos, F., Iordan, A. D., & Dolcos, S. (2011). Neural correlates of emotion–cognition interactions: A review of evidence from brain imaging investigations. *Journal of Cognitive Psychology*, 23(6), 669–694.
- Ernst, M., Nelson, E. E., McClure, E. B., Monk, C. S., Munson, S., Eshel, N., Zarah, E., Leibenluft, E., Zametkin, A., Towbin, K., Blair, J., Charney, D., & Pine, D. S. (2004). Choice selection and reward anticipation: An fMRI study. *Neuropsychologia*, 42(12), 1585–1597. <https://doi.org/10.1016/j.neuropsychologia.2004.05.011>
- Euston, D. R., Gruber, A. J., & McNaughton, B. L. (2012). The role of medial prefrontal cortex in memory and decision making. *Neuron*, 76(6), 1057–1070.
- Fecteau, S., Pascual-Leone, A., Zald, D. H., Liguori, P., Théoret, H., Boggio, P. S., & Fregni, F. (2007). Activation of prefrontal cortex by transcranial direct current stimulation reduces appetite for risk during ambiguous decision making. *The Journal of Neuroscience*, 27(23), 6212–6218.
- Fellows, L. K., & Farah, M. J. (2007). The role of ventromedial prefrontal cortex in decision making: Judgment under uncertainty or judgment per se? *Cerebral Cortex*, 17(11), 2669–2674.
- Fukunaga, R., Brown, J. W., & Bogg, T. (2012). Decision making in the balloon analogue risk task (BART): Anterior cingulate cortex signals loss aversion but not the infrequency of risky choices. *Cognitive, Affective, & Behavioral Neuroscience*, 12(3), 479–490.
- Helfinstein, S. M., Schonberg, T., Congdon, E., Karlsgodt, K. H., Mumford, J. A., Sabb, F. W., Cannon, T. D., London, E. D., Bilder, R. M., & Poldrack, R. A. (2014). Predicting risky choices from brain activity patterns. *Proceedings of the National Academy of Science*, 111(7), 2470–2475. <https://doi.org/10.1073/pnas.1321728111>
- Holroyd, C. B., & Coles, M. G. (2002). The neural basis of human error processing: Reinforcement learning, dopamine, and the error-related negativity. *Psychological Review*, 109(4), 679–709. <https://doi.org/10.1037/0033-295X.109.4.679>
- Kahnt, T., Heinzle, J., Park, S. Q., & Haynes, J.-D. (2010). The neural code of reward anticipation in human orbitofrontal cortex. *Proceedings of the National Academy of Sciences*, 107(13), 6010–6015.
- Kaller, C. P., Rahm, B., Spreer, J., Weiller, C., & Unterrainer, J. M. (2011). Dissociable contributions of left and right dorsolateral prefrontal cortex in planning. *Cerebral Cortex*, 21(2), 307–317. <https://doi.org/10.1093/cercor/bhq096>
- Knutson, B., Adams, C. M., Fong, G. W., & Hommer, D. (2001). Anticipation of increasing monetary reward selectively recruits nucleus accumbens. *The Journal of Neuroscience*, 21(16), RC159.
- Knutson, B., Fong, G. W., Adams, C. M., Varner, J. L., & Hommer, D. (2001). Dissociation of reward anticipation and outcome with event-related fMRI. *Neuroreport*, 12(17), 3683–3687.
- Knutson, B., & Greer, S. M. (2008). Anticipatory affect: Neural correlates and consequences for choice. *Philosophical Transactions of the Royal Society, B: Biological Sciences*, 363(1511), 3771–3786.



- Kohno, M., Ghahremani, D. G., Morales, A. M., Robertson, C. L., Ishibashi, K., Morgan, A. T., Mandelkern, M. A., & London, E. D. (2015). Risk-taking behavior: Dopamine D2/D3 receptors, feedback, and frontolimbic activity. *Cerebral Cortex*, *25*(1), 236–245.
- Kohno, M., Morales, A. M., Ghahremani, D. G., Hellemann, G., & London, E. D. (2014). Risky decision making, prefrontal cortex, and mesocorticolimbic functional connectivity in methamphetamine dependence. *JAMA Psychiatry*, *71*(7), 812–820.
- Koob, G. (1996). Hedonic valence, dopamine and motivation. *Molecular Psychiatry*, *1*(3), 186–189.
- Korucuoglu, O., Harms, M. P., Astafiev, S. V., Kennedy, J. T., Golosheykin, S., Barch, D. M., & Anokhin, A. P. (2020). Test-retest reliability of fMRI-measured brain activity during decision making under risk. *NeuroImage*, *214*, 116759.
- Kurth, F., Zilles, K., Fox, P. T., Laird, A. R., & Eickhoff, S. B. (2010). A link between the systems: Functional differentiation and integration within the human insula revealed by meta-analysis. *Brain Structure & Function*, *214*(5–6), 519–534. <https://doi.org/10.1007/s00429-010-0255-z>
- Lauriola, M., Panno, A., Levin, I. P., & Lejuez, C. W. (2013). Individual differences in risky decision making: A meta-analysis of sensation seeking and impulsivity with the balloon analogue risk task. *Journal of Behavioral Decision Making*, *1*(27), 20–36. <https://doi.org/10.1002/bdm.1784>
- Lejuez, C., Aklin, W. M., Jones, H. A., Richards, J. B., Strong, D. R., Kahler, C. W., & Read, J. P. (2003). The balloon analogue risk task (BART) differentiates smokers and nonsmokers. *Experimental and Clinical Psychopharmacology*, *11*(1), 26–33. <https://doi.org/10.1037/1064-1297.11.1.26>
- Lejuez, C., Aklin, W. M., Zvolensky, M. J., & Pedulla, C. M. (2003). Evaluation of the balloon analogue risk task (BART) as a predictor of adolescent real-world risk-taking behaviours. *Journal of Adolescence*, *26*(4), 475–479.
- Lejuez, C., Read, J. P., Kahler, C. W., Richards, J. B., Ramsey, S. E., Stuart, G. L., Strong, D. R., & Brown, R. A. (2002). Evaluation of a behavioral measure of risk taking: The balloon analogue risk task (BART). *Journal of Experimental Psychology: Applied*, *8*(2), 75. <https://doi.org/10.1037/1076-898X.8.2.75>
- Li, X., Pan, Y., Fang, Z., Lei, H., Zhang, X., Shi, H., Ma, N., Raine, P., Wetherill, R., & Kim, J. J. (2020). Test-retest reliability of brain responses to risk-taking during the balloon analogue risk task. *NeuroImage*, *209*, 116495.
- Maldjian, J. A., Laurienti, P. J., & Burdette, J. H. (2004). Precentral gyrus discrepancy in electronic versions of the Talairach atlas. *NeuroImage*, *21*(1), 450–455. <https://doi.org/10.1016/j.neuroimage.2003.09.032>
- Maldjian, J. A., Laurienti, P. J., Kraft, R. A., & Burdette, J. H. (2003). An automated method for neuroanatomic and cytoarchitectonic atlas-based interrogation of fMRI data sets. *NeuroImage*, *19*(3), 1233–1239. [https://doi.org/10.1016/s1053-8119\(03\)00169-1](https://doi.org/10.1016/s1053-8119(03)00169-1)
- Malvaez, M., & Wassum, K. M. (2018). Regulation of habit formation in the dorsal striatum. *Current Opinion in Behavioral Sciences*, *20*, 67–74.
- Manes, F., Sahakian, B., Clark, L., Rogers, R., Antoun, N., Aitken, M., & Robbins, T. (2002). Decision-making processes following damage to the prefrontal cortex. *Brain*, *125*(3), 624–639.
- Markett, S., Heeren, G., Montag, C., Weber, B., & Reuter, M. (2016). Loss aversion is associated with bilateral insula volume. A voxel based morphometry study. *Neuroscience Letters*, *619*, 172–176.
- Matthews, S. C., Simmons, A. N., Lane, S. D., & Paulus, M. P. (2004). Selective activation of the nucleus accumbens during risk-taking decision making. *Neuroreport*, *15*(13), 2123–2127.
- McLaren, D. G., Ries, M. L., Xu, G., & Johnson, S. C. (2012). A generalized form of context-dependent psychophysiological interactions (gPPI): A comparison to standard approaches. *NeuroImage*, *61*(4), 1277–1286. <https://doi.org/10.1016/j.neuroimage.2012.03.068>
- Miller, E. K., & Cohen, J. D. (2001). An integrative theory of prefrontal cortex function. *Annual Review of Neuroscience*, *24*(1), 167–202.
- Naqvi, N., Shiv, B., & Bechara, A. (2006). The role of emotion in decision making: A cognitive neuroscience perspective. *Current Directions in Psychological Science*, *15*(5), 260–264. <https://doi.org/10.1111/j.1467-8721.2006.00448.x>
- Oba, T., Katahira, K., & Ohira, H. (2021). A learning mechanism shaping risk preferences and a preliminary test of its relationship with psychopathic traits. *Scientific Reports*, *11*(1), 20853.
- Ollinger, J. M., Shulman, G. L., & Corbetta, M. (2001). Separating processes within a trial in event-related functional MRI – I. The method. *NeuroImage*, *13*(1), 210–217. <https://doi.org/10.1006/nimg.2000.0710>
- Paulus, M. P., Rogalsky, C., Simmons, A., Feinstein, J. S., & Stein, M. B. (2003). Increased activation in the right insula during risk-taking decision making is related to harm avoidance and neuroticism. *NeuroImage*, *19*(4), 1439–1448. [https://doi.org/10.1016/S1053-8119\(03\)00251-9](https://doi.org/10.1016/S1053-8119(03)00251-9)
- Rademacher, L., Salama, A., Gründer, G., & Spreckelmeyer, K. N. (2014). Differential patterns of nucleus accumbens activation during anticipation of monetary and social reward in young and older adults. *Social Cognitive and Affective Neuroscience*, *9*(6), 825–831.
- Rao, H., Kordzykowski, M., Pluta, J., Hoang, A., & Detre, J. A. (2008). Neural correlates of voluntary and involuntary risk taking in the human brain: An fMRI study of the balloon analog risk task (BART). *NeuroImage*, *42*(2), 902–910. <https://doi.org/10.1016/j.neuroimage.2008.05.046>
- Rausch, F., Mier, D., Eifler, S., Esslinger, C., Schilling, C., Schirbeck, F., Englisch, S., Meyer-Lindenberg, A., Kirsch, P., & Zink, M. (2014). Reduced activation in ventral striatum and ventral tegmental area during probabilistic decision-making in schizophrenia. *Schizophrenia Research*, *156*(2–3), 143–149.
- Rausch, F., Mier, D., Eifler, S., Fenske, S., Schirbeck, F., Englisch, S., Schilling, C., Meyer-Lindenberg, A., Kirsch, P., & Zink, M. (2015). Reduced activation in the ventral striatum during probabilistic decision-making in patients in an at-risk mental state. *Journal of Psychiatry and Neuroscience*, *40*(3), 163–173.
- Rolls, E. T., Huang, C.-C., Lin, C.-P., Feng, J., & Joliet, M. (2020). Automated anatomical labelling atlas 3. *NeuroImage*, *206*, 116189. <https://doi.org/10.1016/j.neuroimage.2019.116189>
- Ruge, H., Goschke, T., & Braver, T. S. (2009). Separating event-related BOLD components within trials: The partial-trial design revisited. *NeuroImage*, *47*(2), 501–513. <https://doi.org/10.1016/j.neuroimage.2009.04.075>
- Ruissen, M. I., Overgaauw, S., & de Bruijn, E. R. A. (2018). Being right, but losing money: The role of striatum in joint decision making. *Scientific Reports*, *8*(1), 6711. <https://doi.org/10.1038/s41598-018-24617-3>
- Salamone, J. D., & Correa, M. (2012). The mysterious motivational functions of mesolimbic dopamine. *Neuron*, *76*(3), 470–485.

- Schmidt, S. N. L., Fenske, S. C., Kirsch, P., & Mier, D. (2019). Nucleus accumbens activation is linked to salience in social decision making. *European Archives of Psychiatry and Clinical Neuroscience*, 269(6), 701–712. <https://doi.org/10.1007/s00406-018-0947-6>
- Schonberg, T., Fox, C. R., Mumford, J. A., Congdon, E., Trepel, C., & Poldrack, R. A. (2012). Decreasing ventromedial prefrontal cortex activity during sequential risk-taking: An fMRI investigation of the balloon analog risk task. *Frontiers in Neuroscience*, 6, 80.
- Schultz, W. (2016). Dopamine reward prediction error coding. *Dialogues in Clinical Neuroscience*, 18(1), 23–32. <https://doi.org/10.31887/DCNS.2016.18.1/wschultz>
- Steward, T., Pico-Perez, M., Mata, F., Martinez-Zalacain, I., Cano, M., Contreras-Rodriguez, O., Fernandez-Aranda, F., Yucel, M., Soriano-Mas, C., & Verdejo-Garcia, A. (2016). Emotion regulation and excess weight: Impaired affective processing characterized by dysfunctional insula activation and connectivity. *PLoS One*, 11(3), e0152150.
- Ströhle, A., Stoy, M., Wrase, J., Schwarzer, S., Schlagenhauf, F., Huss, M., Hein, J., Nedderhut, A., Neumann, B., & Gregor, A. (2008). Reward anticipation and outcomes in adult males with attention-deficit/hyperactivity disorder. *NeuroImage*, 39(3), 966–972.
- Telzer, E. H., Fuligni, A. J., Lieberman, M. D., & Galván, A. (2013). The effects of poor quality sleep on brain function and risk taking in adolescence. *NeuroImage*, 71, 275–283.
- Wang, M., Zhang, S., Suo, T., Mao, T., Wang, F., Deng, Y., Eickhoff, S., Pan, Y., Jiang, C., & Rao, H. (2022). Risk-taking in the human brain: An activation likelihood estimation meta-analysis of the balloon analog risk task (BART). *Human Brain Mapping*, 43(18), 5643–5657.
- Walter, B. (2003). MARINA: An easy to use tool for the creation of MAsks for Region of Interest Analyses. The 9th International Conference on Functional Mapping of the Human Brain, June 19–22, 2003, New York, NY.
- Xue, G., Lu, Z., Levin, I. P., & Bechara, A. (2010). The impact of prior risk experiences on subsequent risky decision-making: The role of the insula. *NeuroImage*, 50(2), 709–716.
- Yamakawa, K., Ohira, H., Matsunaga, M., & Isowa, T. (2016). Prolonged effects of acute stress on decision-making under risk: A human psychophysiological study. *Frontiers in Human Neuroscience*, 10, 444.
- Zink, C. F., Pagnoni, G., Martin-Skurski, M. E., Chappelow, J. C., & Berns, G. S. (2004). Human striatal responses to monetary reward depend on saliency. *Neuron*, 42(3), 509–517.

**How to cite this article:** Schmidt, S. N. L., Sehrig, S., Wolber, A., Rockstroh, B., & Mier, D. (2024). Nothing to lose? Neural correlates of decision, anticipation, and feedback in the balloon analog risk task. *Psychophysiology*, 61, e14660. <https://doi.org/10.1111/psyp.14660>